

Wright State University

CORE Scholar

---

[Browse all Theses and Dissertations](#)

[Theses and Dissertations](#)

---

1999

## Synthesis of Benzoxazoles Containing Allyl Crosslinking Sites via Claisen Rearrangements

Leslie K. Hutson  
*Wright State University*

Follow this and additional works at: [https://corescholar.libraries.wright.edu/etd\\_all](https://corescholar.libraries.wright.edu/etd_all)

 Part of the [Chemistry Commons](#)

---

### Repository Citation

Hutson, Leslie K., "Synthesis of Benzoxazoles Containing Allyl Crosslinking Sites via Claisen Rearrangements" (1999). *Browse all Theses and Dissertations*. 1.  
[https://corescholar.libraries.wright.edu/etd\\_all/1](https://corescholar.libraries.wright.edu/etd_all/1)

This Thesis is brought to you for free and open access by the Theses and Dissertations at CORE Scholar. It has been accepted for inclusion in Browse all Theses and Dissertations by an authorized administrator of CORE Scholar. For more information, please contact [library-corescholar@wright.edu](mailto:library-corescholar@wright.edu).

SYNTHESIS OF BENZOXAZOLES CONTAINING PENDANT ALLYL  
CROSSLINKING SITES VIA CLAISEN REARRANGEMENTS

A thesis submitted in partial fulfillment  
of the requirements for the degree of  
Master of Science

By

LESLIE K. HUTSON  
B.S., Wright State University, 1994

1999  
Wright State University

WRIGHT STATE UNIVERSITY  
SCHOOL OF GRADUATE STUDIES

August 1, 1999

I HEREBY RECOMMEND THAT THE THESIS PREPARED UNDER MY  
SUPERVISION BY Leslie K. Hutson ENTITLED Synthesis of Benzoxazoles  
Containing Allyl Crosslinking Sites via Claisen Rearrangements BE ACCEPTED IN  
PARTIAL FULFILLMENT OF THE REQUIREMENTS FOR THE DEGREE OF  
Master of Science .

Signed: William A. Feld, Ph.D.  
Thesis CoDirector

Signed: Thuy D. Dang, M.S.  
Thesis CoDirector

Signed: Paul G. Seybold, Ph.D.  
Department Chair

Committee on Final Examination

Signed: Daniel D. Bombick, Ph.D.

Signed: M. Paul Servé, Ph.D.

Signed: William A. Feld, Ph.D.

Approved: Joseph F. Thomas, Jr., Ph.D.  
Dean of the School of Graduate Studies

## ABSTRACT

Hutson, Leslie K. M.S. Department of Chemistry, Wright State University, 1999.  
Synthesis of Benzoxazoles Containing Allyl Crosslinking Sites via Claisen  
Rearrangements.

The reaction of diethyl 2,5-dihydroxyterephthalate with allyl bromide/ $K_2CO_3$  in DMF followed by hydrolysis provided 2,5-di(allyloxy)terephthalic acid. The conversion of 2,5-di(allyloxy)terephthalic acid to 1,4-di(2-benzoxazolyl)-2,5-di(allyloxy)benzene in PPSE was unsuccessful. However, the reaction of 1,4-di(2-benzoxazolyl)-2,5-dihydroxybenzene with allyl bromide/ $K_2CO_3$  provided 1,4-di(2-benzoxazolyl)-2,5-di(allyloxy)benzene. DSC analysis indicated that 1,4-di(2-benzoxazolyl)-2,5-di(allyloxy)benzene undergoes a Claisen rearrangement to the corresponding diallyl product. The synthesis of 2-allyloxy-1,4-di(2-benzoxazolyl)benzene was carried out using 2-hydroxy-1,4-di(2-benzoxazolyl)benzene as starting material. DSC analysis was inconclusive with respect to a Claisen rearrangement. The reaction of 2-allyloxybenzoic acid with 2,2-bis(3-amino-4-hydroxyphenyl)-1,1,1,3,3,3-hexafluoropropane in PPSE was unsuccessful but the reaction of 2,2-bis(2-(2-hydroxyphenyl)-5-benzoxazolyl)-1,1,1,3,3,3-hexafluoropropane with allyl bromide/ $K_2CO_3$  in DMF provided 2,2-bis(2-(2-allyloxyphenyl)-5-benzoxazolyl)-1,1,1,3,3,3-hexafluoropropane. DSC analysis of 2,2-bis(2-(2-allyloxyphenyl)-5-benzoxazolyl)-1,1,1,3,3,3-hexafluoropropane was inconclusive as to the presence of a Claisen rearrangement.

## TABLE OF CONTENTS

	page
ABSTRACT .....	iii
LIST OF FIGURES .....	vi
LIST OF TABLES .....	viii
DEDICATION .....	ix
ACKNOWLEDGMENT .....	x
INTRODUCTION.....	1
HISTORICAL .....	3
Scaling and the RC Delay Problem.....	3
Required Alternative Material Properties.....	4
Factors Affecting k and Tg.....	6
The Nanofoam Approach .....	7
Polyimides .....	9
Aromatic Benzoxazoles.....	11
The Claisen Rearrangement .....	13
EXPERIMENTAL .....	16
Instrumentation and Chemicals .....	16
Diethyl 2,5-di(allyloxy)terephthalate <b>15</b> .....	16
2,5-Di(allyloxy)terephthalic Acid <b>16</b> .....	17
2,5-bis(2-benzoxazolyl)-1,4-di(allyloxy)benzene <b>18</b> .....	17

## TABLE OF CONTENTS (CONTINUED)

	page
2,5-bis(2-benzoxazolyl)-1,4-dihydroxybenzene <b>20</b> .....	18
2,5-bis(2-benzoxazolyl)-1,4-di(allyloxy)benzene <b>18</b> .....	18
2,5-bis(2-benzoxazolyl)-1-hydroxybenzene <b>24</b> .....	19
2,5-bis(2-benzoxazolyl)-1-allyloxybenzene <b>25</b> .....	19
Ethyl 2-allyloxy benzoate <b>28</b> .....	19
2-Allyloxybenzoic acid <b>29</b> .....	20
2,2-Bis(2-(2-allyloxyphenyl)-5-benzoxazolyl)-1,1,1,3,3,3-hexafluoropropane <b>31</b> .....	20
2,2-Bis(2-(2-hydroxyphenyl)-5-benzoxazolyl)-1,1,1,3,3,3-hexafluoropropane <b>33</b> .....	21
2,2-Bis(2-(2-allyloxyphenyl)-5-benzoxazolyl)-1,1,1,3,3,3-hexafluoropropane <b>31</b> .....	21
Thermal Analysis .....	22
RESULTS AND DISCUSSION .....	23
Diallyloxybenzoxazole Model Compound Synthesis .....	23
Monoallyloxybenzoxazole Model Compound Synthesis .....	26
6F-benzoxazole Model Compound Synthesis .....	27
Thermally Induced Claisen Rearrangement .....	32
REFERENCES .....	46
VITA .....	47

## LIST OF FIGURES

Figure		Page
1.	Voids Remain After Thermolysis of Labile Block in Nanofoams.....	8
2.	Possible Void Shapes Resulting from Labile Block Composition. ....	8
3.	T <sub>g</sub> vs % Hydroxy in Polymers <b>9</b> (3-6).....	12
4.	IR spectrum of 2,5-dihydroxyterephthalate .....	35
5.	IR spectrum of diethyl 2,5-dihydroxyterephthalate .....	35
6.	IR spectrum of 2,5-di(allyloxy)terephthalic acid.....	36
7.	IR spectrum of 2,5-bis(2-benzoxazolyl)-1,4-dihydroxybenzene .....	36
8.	IR spectrum of 2,5-bis(2-benzoxazolyl)-1,4-di(allyloxy)benzene .....	37
9.	IR spectrum of 2-hydroxyterephthalic acid .....	37
10.	IR spectrum of 2,5-bis(2-benzoxazolyl)-1-hydroxybenzene .....	38
11.	IR spectrum of 2,5-bis(2-benzoxazolyl)-1-allyloxybenzene .....	38
12.	IR spectrum of ethyl salicylate .....	39
13.	IR spectrum of ethyl 2-allyloxy benzoate.....	39
14.	IR spectrum of 2-allyloxybenzoic acid.....	40
15.	IR spectra of 2,2-bis(2-(2-hydroxyphenyl)-5-benzoxazolyl)-1,1,1,3,3,3- hexafluoropropane .....	40
16.	IR spectra of 2,2-bis(2-(2-allyloxyphenyl)-5-benzoxazolyl)-1,1,1,3,3,3- hexafluoropropane .....	41
17.	DSC scan of 2,5-bis(2-benzoxazolyl)-1,4-di(allyloxy)benzene .....	41

## LIST OF FIGURES (CONTINUED)

Figure	Page
18. DSC rescan of 2,5-bis(2-benzoxazolyl)-1,4-di(allyloxy)benzene .....	42
19. TGA in air of 2,5-bis(2-benzoxazolyl)-1,4-di(allyloxy)benzene.....	42
20. DSC scan of IR spectra of 2,2-bis(2-(2-allyloxyphenyl)-5-benzoxazolyl)- 1,1,1,3,3,3-hexaflouropropane .....	43
21. DSC rescan IR spectra of 2,2-bis(2-(2-allyloxyphenyl)-(2-benzoxazolyl)- 1,1,1,3,3,3-hexaflouropropane .....	43
22. TGA in helium of IR spectra of 2,2-bis(2-allyloxyphenyl)-5-benzoxazolyl)- 1,1,1,3,3,3-hexaflouropropane .....	44
23. DSC scan of 2,5-bis(2-benzoxazolyl)-1-allyloxybenzene .....	44
24. DSC rescan of 2,5-bis(2-benzoxazolyl)-1-allyloxybenzene .....	45
25. TGA in air of 2,5-bis(2-benzoxazolyl)-1-allyloxybenzene .....	45



## LIST OF TABLES

Table	Page
1. $T_g$ and $k$ as a Function of Hydroxyl Content for Polymer(s) <b>9</b> .....	13
2. Analytical Results for Diallyloxybenzoxazole Model Compound Synthesis (Compounds <b>15</b> , <b>16</b> , <b>18</b> , and <b>20</b> ).....	26
3. Analytical Results for Monoallyloxybenzoxazole Model Compound Synthesis. .....	28
4. Analytical Results for 6F-allyloxybenzoxazole Synthesis .....	31
5. Elemental Analysis Results for Benzoxazole Model Compounds and Precursors .....	31

## **DEDICATION**

Dedicated to my parents, Karen and Kyle Hutson, for their infinite love, support and encouragement.

## **ACKNOWLEDGMENT**

I would like to express my sincere gratitude to Dr. Fred Arnold for providing the opportunity and encouragement, to Mr. Thuy Dang for extending his expertise and guidance and to Dr. William Feld for his advice and efforts throughout this project.

## INTRODUCTION

There is an ever present demand for smaller, faster, and more efficient electronic devices. In order to keep up with this demand, designers must try to pack more circuitry into an increasingly smaller unit area. There are two logical ways of achieving this. One is to stack chips on top of one another, creating wafers with multilayer wiring, currently 6-8 layers in thickness.<sup>1</sup> Another is to decrease the space between conducting elements, shrinking the entire chip size. The current goal is to have chips with devices smaller than 0.18  $\mu\text{m}$  by the year 2001.<sup>2</sup>

When circuitry becomes more densely packed the slight ability of the currently used insulating material to conduct an electric charge can result in performance problems such as crosstalk, power dissipation, and delay within the microelectronic chip. Silicon dioxide (recall the infamous Silicon Valley, California) has been the insulating material used thus far. Unfortunately, this material will no longer be suitable for use in the future microstructures due to its relatively high dielectric constant. New materials must be developed with superior capabilities to act as insulating materials between conducting features in these shrinking microelectronic circuits.

Polymers have been a natural choice for replacement materials due to their ease of processing and high temperature capabilities, which are required during the manufacturing process. The challenge has been to produce polymers with the combination of all of the required thermal, mechanical, electrical, and chemical properties necessary to make them realistic replacement candidates. From the long list of

requirements, a low dielectric constant and a high  $T_g$  have been identified as the most crucial sought after properties.

The most widely accepted and studied group to have the potential to possess these qualities are the polyimides, but benzoxazoles have also recently been considered as possible replacement candidates. Unlike the polyimides, benzoxazoles exhibit lower dielectric constants and lower moisture uptake (less than 1%), but show poorer solvent resistance.<sup>3</sup>

The main objectives of this research were to 1) generate benzoxazole model compounds containing pendant allyloxy groups, 2) carry out a Claisen rearrangement that would provide a hydroxyl hydrogen bonding site and an allyl crosslinking site, and 3) characterize the model compounds and related products using Infrared Spectroscopy (IR),  $^1\text{H}$  and  $^{13}\text{C}$  Nuclear Magnetic Resonance (NMR), Differential Scanning Calorimetry (DSC), and Thermogravimetric Analysis (TGA).

## HISTORICAL

### Scaling and the RC Delay Problem

Microprocessor performance is typically improved by decreasing the device size. This has led to an increase in the number of wiring levels as well as a reduction in the wiring pitch, which is the sum of the metal line width and the width of the spacing between lines. This allows greater device speed, an increase in the device packing density, and an increase in the number of functions that can reside on a single chip.

The increased packing density requires a much larger number of metal interconnects. Below device dimensions of  $0.25\mu\text{m}$  a major performance barrier is encountered due to resistance-capacitance (RC) delay of the metal interconnects.<sup>4</sup> The interconnect RC delay increases roughly quadratically with decreasing feature size.<sup>5</sup> Although the speed of the device will increase as feature size decreases, the interconnect delay becomes the major fraction of the total delay and limits improvement in device performance. The time delay associated with the interconnects is dependent on the resistance of the metal, and the capacitance of the insulating dielectric media. Since the resistance is given by:

$$R = \rho \frac{L}{A}$$

where  $\rho$  is the resistivity,  $L$  is the length, and  $A$  is the cross sectional area of the wire, one can see that as the area ( $A$ ) of the metal lines decreases, the resistance increases.<sup>6</sup> The current material used for the metal lines is generally an Al(Cu) alloy, but recently it has been shown that Cu can be used alone.<sup>4</sup> Copper has the advantage of having a lower

resistance, but requires higher processing temperatures. Also, from the equation for capacitance:

$$C = \frac{Q}{V} = \frac{\epsilon A}{s}$$

where Q is the charge, V is the potential difference across parallel plates, A is the area of the plates, s is the plate separation, and  $\epsilon$  is the permittivity of the dielectric media, it can be seen that as the space between the metal lines (acting as parallel plate capacitors) decreases, the capacitance increases.<sup>6</sup> The permittivity,  $\epsilon$ , is expressed as:

$$\epsilon = k\epsilon_o$$

where  $\epsilon_o$  is the permittivity of free space, and k is the dielectric constant. It should be noted then that the dielectric constant directly effects the capacitance. A lower dielectric constant provides a lower capacitance, and it must be decreased in order to compensate for the increase in capacitance caused by a decrease in the spacing between metal lines.

It is obvious that the chips of the future will require lower resistivity conductors such as copper, and the introduction of low dielectric constant (k) materials as interlayer dielectrics (ILDs) to overcome the resistance-conductance (RC) coupling problem.

### **Required Alternative Material Properties**

There is a long list of physical and chemical properties required of new low-dielectric materials suitable for ILD applications.

Electrical requirements include a low dielectric constant ( $k < 3$ ), low dielectric loss, and high breakdown voltage.<sup>2,7</sup> Of these, the dielectric constant is considered the most important feature, because the problems of propagation delay and crosstalk noise are determined primarily by k. The current SiO<sub>2</sub> film has a k of approximately 4.<sup>4</sup> The goal is

to obtain a material with a  $k$  value of 2.0 - 2.4 by the year 2001, with continuing decreases further into the future.<sup>3</sup>

High thermal stability is also a must for future ILDs in order to be compatible with lead bath processing, and with the use of Cu metal lines. The fabrication process may require as many as 10 - 15 temperature excursions (thermal cycling), where temperatures may reach 400 - 450°C.<sup>4</sup> These factors require a material with a  $T_g$  greater than or equal to the highest processing temperature, the target  $T_g$  being higher than 400°C.<sup>2</sup> The  $T_g$  must, of course, also be lower than the decomposition temperature ( $T_d$ ). Due to the thermal cycling and the high processing temperatures, a low coefficient of thermal expansion (CTE) is also required ( $< 50\text{ppm}/^\circ\text{C}$ ).<sup>2</sup> High CTEs result in a mismatch between the ILDs and metal substrates, which can result in delamination if the adhesion is poor. Adhesion requirements include no peeling between ILD/ILD interfaces after 450°C thermal cycles.<sup>2</sup>

The candidate ILD materials must also be durable, and thus have certain mechanical requirements. Among them are a large Young's modulus, ( $E$ ), ( $>1\text{GPa}$ ), and elongation-at-break ( $>5\%$ ).<sup>2</sup> The ability to produce uniform thin film thickness, as well as having good gap fill (no voids at  $0.35\mu\text{m}$ ) is also important.<sup>2</sup>

Finally, there are chemical considerations. The ILD material must be resistant to acids, bases, and strippers used in processing. Additionally, they must have low moisture uptake ( $<2\%$ ).<sup>2</sup> Moisture uptake must be kept to a minimum because of the large  $k$  of water, 78.5 at 25°C.<sup>4</sup> Because the  $k$  of water is so large, it can have detrimental effects on the  $k$  of the material if it is present even in small concentrations.



## Factors Affecting $k$ and $T_g$

Since the value of  $k$  relates to the polarizability of a material, it is strongly dependent on the chemical structure. Saturated hydrocarbons are much less polarizable than species that are unsaturated, conjugated, or that have polarizable phenyl groups. Therefore, single bonded structures will offer the lowest  $k$  values. Unfortunately, aliphatic C-C, C-H, and C-N bonds generally become unstable at temperatures above 400°C, which are required during the manufacturing process.<sup>4</sup> Only organic materials with non-aliphatic C-C, C-O, C-N, C-S, aromatics, and crosslinked or ladder structures are generally capable of withstanding these elevated processing temperatures. Because of the polarizability of these structures, these chemical features that impart good thermal stability generally tend to increase  $k$  in the process. Furthermore, it has been shown that the greater the number of fused rings along the polymer backbone, the higher the  $T_g$  will be.<sup>3</sup> Since it is required to have a high  $T_g$ , but a low  $k$ , it seems that these two properties are at odds with one another such that the chemical architectures that help decrease  $k$  values, also decrease  $T_g$  values, and vice versa.

A few useful approaches have been found to help alleviate this problem. Thermal stability can be enhanced without increasing the number of fused rings by crosslinking a polymer because multiple bonds must be broken before degradation can occur. Beyond that, it is accepted that in order to have materials with high enough  $T_g$ 's, non-aliphatic or aromatic groups must make up the bulk of the polymer backbone. It is possible to diminish the increase in  $k$  associated with these groups by breaking them up with C-C single bonds, but this does decrease the thermal stability. The most successful way of decreasing  $k$  seems to be the incorporation of fluorine moieties within the material.

Substitution of H by F or a CF<sub>3</sub> group decreases the electron polarizability due to fluorine's strong electron-withdrawing inductive effects.<sup>4</sup> The bulky CF<sub>3</sub> group is also capable of reducing efficient molecular packing, thus increasing the free volume of the molecule and diffusing the internal dipole. Additionally, since fluorine is very hydrophobic, it has the added benefit of lowering moisture uptake. Fluorination also improves thermal stability because the C-F bond is stronger than the C-H bond.

### **The Nanofoam Approach**

The incorporation of a low dielectric material such as air ( $k = 1$ ) into an existing polymer matrix would have the effect of lowering the bulk dielectric constant of the polymer. The problem with the addition of air or any other material into a polymer to form a foamed system for microelectronic applications is that the pore sizes must be uniform, and smaller than the film thickness and the smallest microelectronic feature (less than 0.5  $\mu\text{m}$ ).<sup>1</sup> Many methods have been utilized to try to produce polymer foams with these required characteristics, such as the use of foaming agents, partial degradation generating foaming agents, inclusion of hollow microspheres, and microwave processing.<sup>1</sup> Most of these methods result in unsuitable uniformity in pore shape, and larger than acceptable pore sizes.

An interesting new approach to polymer foam formation is the use of nanofoam technology which uses a block copolymer approach where there is a thermally labile block and a thermally stable block. Thermolysis of the labile block leaves pores of the size and shape of the degraded labile block as illustrated in Figure 1.

This method also produces pores of very uniform shape, and of acceptable size, on the nanometer range, with the resulting foams termed nanofoams. Nanoporous foams

of 6-200 nm pore size with void volumes from 10 -18 % have been successfully synthesized using this approach.<sup>1,8</sup>

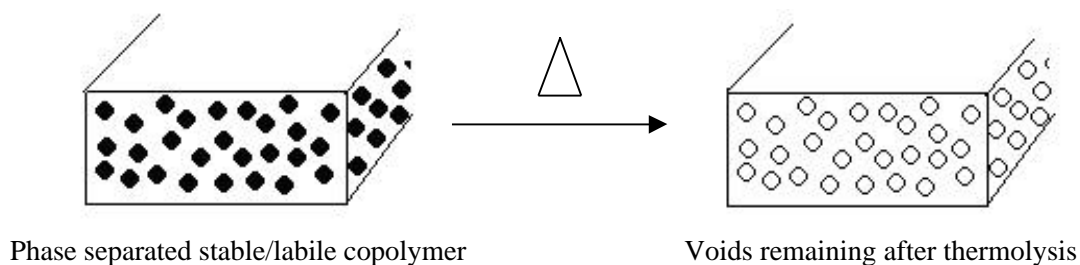


**Figure 1.** Voids Remain After Thermolysis of Labile Block in Nanofoams.

The requirement of having closed, non-interconnected pores limits the amount of labile block to around 30% (vol).<sup>1</sup> Higher levels would result in cylindrical or lamellar domains resulting in interconnected or collapsed structures upon foaming as illustrated in Figure 2, causing inconsistent dielectric properties. The voids or pores must also be closed cell to retard solvent penetration during processing.

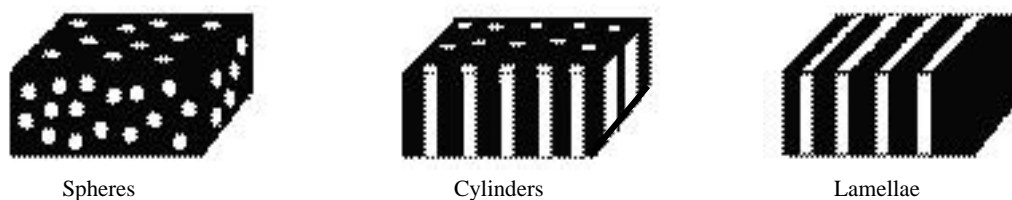
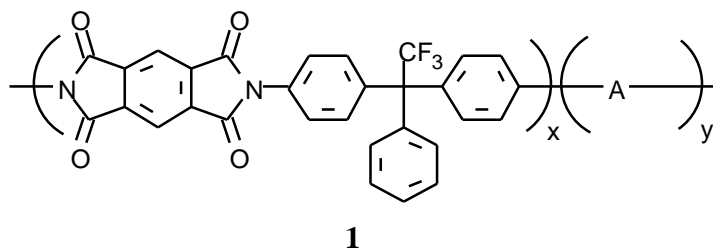


**Figure 2.** Possible Void Shapes Resulting from Labile Block Composition.

Finding suitable labile blocks is a challenge because the labile block must be able to phase separate from the polymer matrix, be thermally stable during film processing, but also must quantitatively degrade during thermolysis. The temperature that the labile block must withstand during processing and the temperature at which it degrades is termed the processing window. This processing window is often 50°C or less, significantly narrowing the field for suitable labile block candidates.<sup>7</sup> Some of the more

commonly used labile blocks are poly (propylene oxide)( PPO), poly (methyl methacrylate) (PMMA), styrenic polymers, and aliphatic polyesters, polyactides, and polycarbonates.<sup>1</sup>

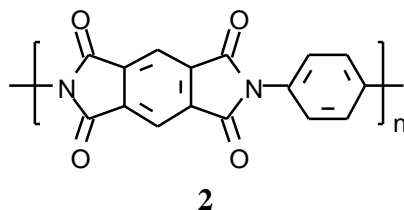


The nanofoam approach was first demonstrated using the triblock copolymers consisting of the stable poly(phenylquinoxaline) (PPQ) block, and PMMA or PPO as the labile block. The resulting PPQ nanofoams showed a reduction in  $k$  from 2.8 to 2.4.<sup>9</sup> Subsequently, the PMDA/3FDA polyimide system **1** has show the most promise as a nanofoam candidate.<sup>1</sup> In this polyimide copolymer system, the labile block (-A-) must withstand curing temperatures of approx. 300°C, and degrade at approx. 350°C.<sup>1</sup> Both PMMA and PPO have been used as the labile blocks in this system, with the PMDA/3FDA copolymer having 24% PPO showing a drop in dielectric constant from 2.85 to 2.2.<sup>1</sup>

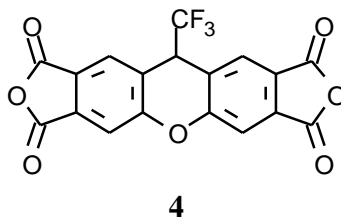
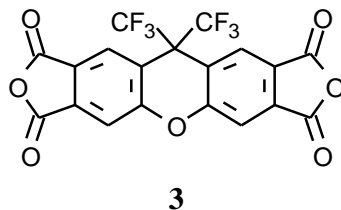
One final requirement for these nanofoams is that they must maintain the physical properties of the parent polymer. If foaming reduces key requirements such as gap filling, tensile strength, or other susceptible mechanical and thermal properties then the reduction in  $k$  that is gained is not worth the loss of the other properties.

### Polyimides

Prior to their use in nanofoams, polyimides **2** were researched as candidate low-dielectric materials due to their intrinsically low dielectric constants ( $k= 3.1\pm .4$ ), high

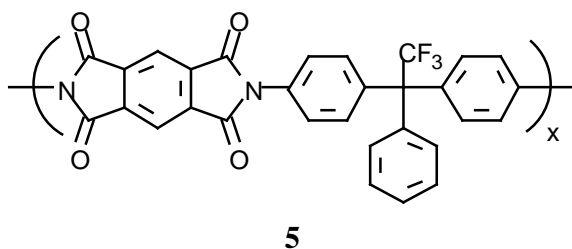


$T_g$ 's, ease of processing, availability, solvent resistance, and excellent mechanical properties.<sup>7,9</sup> The latter two properties can be attributed in part to the ordering of the polymer and the alignment of chains parallel to the surface. Unfortunately, this ordering can cause poor planarization, resulting in an anisotropic dielectric constant, with the in-plane dielectric constant much greater than the commonly measured out-of-plane dielectric constant.<sup>9</sup> The incorporation of pendant perfluoroalkyl groups has been the method of choice employed to make polyimides with lower, more isotropic dielectric constants, with values of  $k$  having been reported as low as 2.5 in polyimides derived from 6FXDA **3** and 3FXDA **4**.<sup>1</sup>



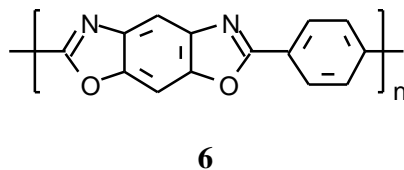
The current best candidate is the condensation polyimide PMDA/3FDA **5** made from pyromellitate dianhydride (PMDA) and 1,1-bis(4-aminophenyl)-1-phenyl-2,2,2-

trifluoroethane (3FDA), due to its low  $k$  (2.8), very high  $T_g$  (approx 430°C), and high  $T_d$  of 500°C.<sup>1</sup>



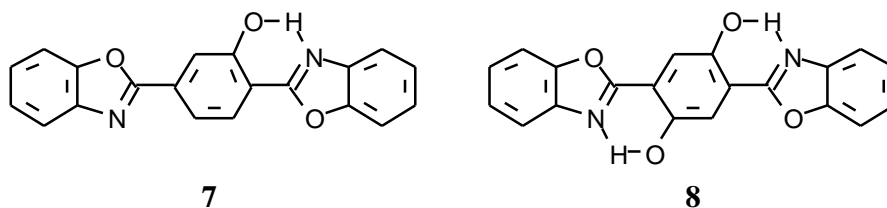
### Aromatic Benzoxazoles

Aromatic benzoxazoles **6** also possess favorable physical properties for low dielectric applications.<sup>10</sup> Compared to the unsubstituted polyimides, unaltered



benzoxazoles have  $k = 3.0$  (vs. 3.4 for polyimide), and a lower moisture uptake (<1%, vs. 3.4 % for polyimides), as well as similar high thermal and mechanical performance to the polyimides.<sup>10</sup> Both of these unsubstituted parent compounds have  $T_g$ 's greater than  $T_d$ . As with the polyimides, the incorporation of perfluoroisopropyl groups along the backbone structure serves to decrease the  $k$  significantly. Unfortunately, the incorporation of fluorine containing groups along the polymer backbone breaks up the number of fused rings, which leads to the unwanted decrease in the  $T_g$ . In order to retain a high  $T_g$ , the generation of intramolecular hydrogen bonding is accomplished by incorporating pendant hydroxyl groups that can hydrogen bond with the nitrogen of the benzoxazole heterocycle as shown for benzoxazoles **7** and **8**.<sup>3</sup>

A single hydroxyl group is capable of forming a 4-fused-ring structure **7**, and the addition of another hydroxyl group provides a 7-fused-ring structure **8** when incorporated in PBO polymers.<sup>3</sup>



The  $T_g$  remains a function of the stability of hydrogen bonding up to 400°C as indicated in Table 1 and Figure 3.<sup>10</sup> Figure 3 is a simple graphical representation illustrating from DSC analysis that  $T_g$  increases with increasing hydroxyl mol percent in mono-hydroxy 6F-PBO polymers.

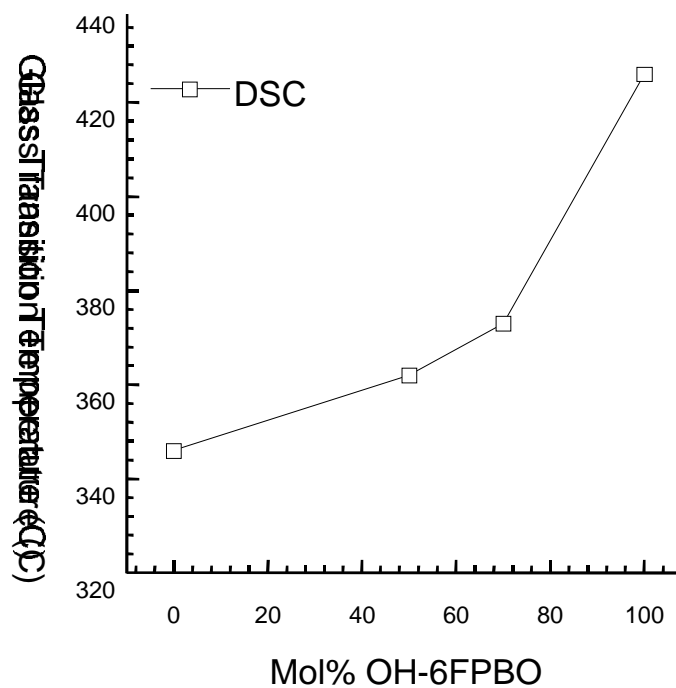


**Figure 3.**  $T_g$  vs % Hydroxy in Polymers **9** (3-6).

Table 1 shows a series of 6FPBO homopolymers and copolymers **9** with varying percentages of CF<sub>3</sub> and hydroxyl groups, synthesized to determine the best combination of the two functionalities to retain both high T<sub>g</sub> and low k values.

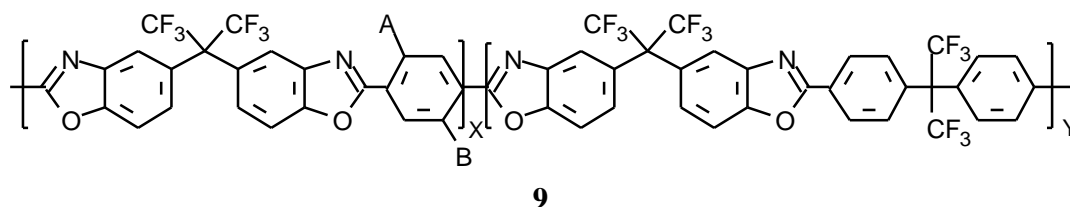


**Table 1.** T<sub>g</sub> and k as a Function of Hydroxyl Content for Polymer(s) **9**.

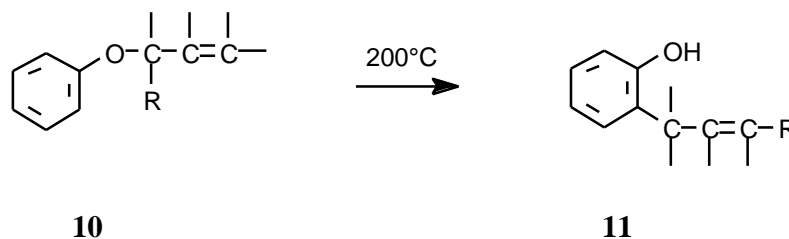
Polymer Number	A	B	X	Y	[η]	T <sub>g</sub> <sup>a</sup> (°C)	T <sub>g</sub> <sup>b</sup> (°C)	K (100Hz)	k (10KHz)	k (1MHz)
1	-H	-H	0	10	2.30	325	315	2.41	2.36	2.32
2			50	50	1.37	346	336	2.68	2.64	2.59
3	-OH	-H	100	0	2.06	426	390	2.38	2.37	2.35
4			90	10	1.30	415	410	2.49	2.46	2.42
5			70	30	2.34	373	371	2.14	2.12	2.09
6			50	50	1.35	362	353	2.23	2.19	2.15
7	-OH	-OH	100	0	3.10	>450	454	3.02	2.95	2.88
8			75	25	1.34	>450	—			—
9			50	50	0.88	>450	430	3.14	3.04	2.95
10			25	75	0.47	>450	332			—

<sup>a</sup>Differential Scanning Calorimeter, <sup>b</sup>Dynamic Mechanical Analysis.

### The Claisen Rearrangement

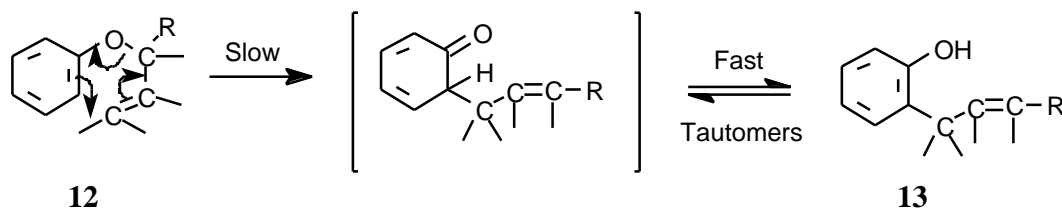
Allylic aryl ethers **10** rearrange to o-allylphenols **11** upon heating in the Claisen rearrangement.<sup>11</sup> If both ortho positions are filled, the allylic group will migrate to the para position.<sup>11</sup> There is no reaction when both the ortho and para positions are filled. In the ortho migration the allylic group always undergoes an allylic shift. That is, as shown





above, a substituent (R) to the oxygen is now to the ring (and vice versa). On the other hand, in the para migration there is never an allylic shift. The allylic group is found exactly as it was in the original ether.

The mechanism of the Claisen rearrangement has been shown to be a concerted pericyclic [3,3] sigmatropic rearrangement.<sup>11</sup>



With the ortho rearrangement, evidence for this mechanism is the lack of a catalyst, the fact that the reaction is first order in the ether, the absence of crossover products when mixtures are heated, and the presence of the allylic shift, which is required by the mechanism.<sup>11</sup> The allylic shift for the ortho rearrangement (and the absence of one for the para) has been demonstrated by C<sup>14</sup> labeling, even when no substituents are present.<sup>11</sup> Ethers with alkyl groups in the  $\gamma$  position (ArO-C-C=C-R) sometimes give abnormal products, with the  $\gamma$  carbon becoming attached to the ring.<sup>11</sup> This occurs due to a further rearrangement of the normal product.

The Claisen rearrangement does not involve ions, so it should not be greatly dependent on the presence or absence of substituent groups on the ring. Electron donating

groups increase the rate of the reaction and electron withdrawing groups decrease it, but the effect is small, with studies showing the p-amino compound reacting only 10-20 times faster than the p-nitro compound.<sup>11</sup> Solvent effects are great, with rates varying over a 300 fold range in 17 different solvents.<sup>11</sup>

The main objectives of this research were to 1) generate benzoxazole model compounds containing pendant allyloxy groups, 2) carry out a Claisen rearrangement that would provide a hydroxyl hydrogen bonding site and an allyl crosslinking site, and 3) characterize the model compounds and related products using Infrared Spectroscopy (IR), <sup>1</sup>H and <sup>13</sup>C Nuclear Magnetic Resonance (NMR), Differential Scanning Calorimetry (DSC), and Thermogravimetric Analysis (TGA).

## EXPERIMENTAL

### Instrumentation and Chemicals

Infrared spectra (IR) were obtained with a Bruker IFS 28 using KBr pellets or thin films. Elemental analyses were performed by ChemSys Inc. at Wright Patterson Air Force Base. A Finnegan 4500 Mass spectrometer was used to obtain mass spectra (solid state), performed by ChemSys Inc. as well. Differential scanning calorimetry (DSC) and thermogravimetric analyses (TGA) were performed by MLBP, Wright Patterson Air Force Base on a TA Instruments DSC 2910 and a TA Instruments TGA 2950 respectively. Melting points were obtained from a MelTemp capillary melting point apparatus and used without correction. All starting materials were purchased from Aldrich Chemical Company, with the exception of 2,2-bis(3-amino-4-hydroxyphenyl)-1,1,1,3,3,3-hexafluoropropane which was purchased from DayChem Laboratories. All reagents were used without further purification.

### Diethyl 2,5-diallyloxyterephthalate (**15**)

In a 500 mL, 3 necked, round-bottomed flask equipped with reflux condenser was placed 17.43g (0.037 mol) of diethyl 2,5-dihydroxyterephthalate **14**, 11.15g (0.076 mol) of K<sub>2</sub>CO<sub>3</sub>, and 190 mL of DMF. The mixture was stirred under nitrogen for 30 min. Allyl bromide, 11.60g (0.096 mol) was added and the reaction mixture was heated at 50°C for 2 days until complete by TLC (silica, 25:75 heptane/methylene chloride). The mixture was poured over ice (1000 mL) and the resulting precipitate was filtered and air dried. The precipitate was recrystallized from hexanes, filtered, and dried under vacuum to yield

14g of crude product. Because the melting point range was very wide, the crude material was chromatographed on silica (25/75 heptane/methylene chloride). Solvent was removed under vacuum to provide 11 g (48%) of pale-yellow needles: mp = 40–1°C; IR (KBr)  $\text{cm}^{-1}$  3068 (aromatic C-H), 2980-2864 (aliphatic C-H), 1705 (C=O), 1650 (alkene C=C), 1508, 1459 (aromatic C=C), 1201 (C-O-C); MS  $m/z$  ( $M^+$ ) = 334. Anal. Calcd. for  $\text{C}_{18}\text{H}_{22}\text{O}_6$ : C, 64.66%; H, 6.63%. Found: C, 64.55%; H, 6.65%.

### **2,5-Di(allyloxy)terephthalic Acid (16)**

In a 500 mL 3-necked, round-bottomed flask with reflux condenser was placed 5.4g (0.0162 mol) of diethyl 2,5-di(allyloxy)terephthalate **15**, 3.5g (0.0875 mol) of NaOH, and 100 mL of a 50/50 (vol) ethanol/water solution. The reaction was heated at reflux overnight. Ethanol was removed *in vacuo* and the solution was diluted with 20 mL of water. The product was precipitated by adding HCl dropwise until a pH of 1. The product was filtered, washed with copious amounts of water and air dried. The product was recrystallized from xylene, filtered, and dried *in vacuo* to yield 3.6g (80%) of yellow product: mp 168-70°C; IR (KBr)  $\text{cm}^{-1}$  3250-2250 (O-H), 1675 (C=O), 1447, 1502 (aromatic C=C), 1249, 1216 (C-O-C); MS  $m/z$  ( $M^+$ ) = 278. Anal. Calcd. For  $\text{C}_{14}\text{H}_{14}\text{O}_6$ : C, 60.43%; H, 5.07%. Found: C, 60.33%; H, 4.81%.

### **2,5-bis(2-benzoxazolyl)-1,4-di(allyloxy)benzene (18)**

In a polymerization flask equipped with an overhead stirrer and nitrogen inlet/outlet, was placed 1.00g (0.0036 mol) of 2,5 di(allyloxy)terephthalic acid **16**, 0.785g (0.0072 mol) of 2-aminophenol **17**, 2.67g (0.0144 mol) tributylamine, 8.64g trimethylsilyl polyphosphate, and 22 mL of o-dichlorobenzene. The mixture was stirred

and heated at 140°C for 24 h, and 165°C for 6 h. No product was obtained by precipitation.

#### **2,5-bis(2-benzoxazolyl)-1,4-dihydroxybenzene (20)**

In a polymerization flask equipped with an overhead stirrer and a nitrogen inlet and outlet, was placed 8.0g (0.0403 mol) of 2,5-dihydroxyterephthalic acid **19**, 8.813g (0.0808 mol) of 2-aminophenol **17**, and 40g of 83% poly(phosphoric acid). The mixture was stirred and heated at 160°C overnight. The product was precipitated from water, filtered and washed with copious amounts of water to achieve neutral pH. The product was filtered and air dried before being recrystallized from o-dichlorobenzene to yield 5.73g (41%) of yellow powder: mp 380-3°C; IR (KBr)  $\text{cm}^{-1}$  3129 (O-H), 1566 (C=N), 1502, 1451 (aromatic C=C), 1230 (C-O-C); Mass spectra (m/z)  $M^+ = 334$ .

#### **2,5-bis(2-benzoxazolyl)-1,4-di(allyloxy)benzene (18)**

In a 3-necked, round-bottomed flask equipped with a Dean-Stark trap and a condenser, was placed 1.85g (0.0054 mol) of 2,5-bis(2-benzoxazolyl)-1,4-dihydroxybenzene **20**, 0.432g (0.0108 mol) of NaOH, 50 mL of toluene, and 100 mL of DMF. The reaction mixture was heated at 115°C for 2 h until the required amount of water was distilled. The flask was cooled to rt, and 1.70g (0.014 mol) of allyl bromide was added and the mixture was heated at 50°C for 2 d. The product was precipitated with ice (500 mL). The solid was filtered and air dried before being recrystallized from methylene chloride to yield 1.17g (51%) of pale yellow product: mp 222-3°C; IR (KBr)  $\text{cm}^{-1}$  3059, 3012 (aromatic C-H), 2863 (aliphatic C-H), 1678 (alkene C=C), 1552 (C=N), 1453, 1426 (aromatic C=C), 1225 (C-O-C); MS m/z ( $M^+$ ) = 424. Anal. Calcd. for  $\text{C}_{26}\text{H}_{20}\text{N}_2\text{O}_4$ : C, 73.60%; H, 4.75%; N, 6.60%. Found: C, 72.97%; H, 4.63%; N, 6.42%.

### **2,5-bis(2-benzoxazolyl)-1-hydroxybenzene (24)**

In a polymerization flask equipped with an overhead stirrer and nitrogen inlet and outlet, was added 2.0g (0.011 mol) of 2-hydroxyterephthalic acid **23**, 2.41g (0.0221 mol) of 2-aminophenol **17**, and 33g of 83% poly(phosphoric acid). The mixture was stirred at 160°C overnight, and then precipitated in water. It was washed with copious amounts of water to achieve neutral pH, then filtered and air dried before being recrystallized from o-dichlorobenzene to give 2.32g (64%) pale yellow product: mp 318-21°C; IR (KBr)  $\text{cm}^{-1}$  3048 (O-H), 1566 (C=N), 1496, 1452 (aromatic C=C), 1247 (C-O-C); MS m/z (M+) = 328.

### **2,5-bis(2-benzoxazolyl)-1-allyloxybenzene (25)**

To a 250 mL roundbottomed flask equipped with a Dean-Starks trap and a condenser, was added 1.90g (0.0058 mol) of 2,5-bis(2-benzoxazolyl)-1-hydroxybenzene **24**, 0.243g (0.0061 mol) NaOH, 50 mL of toluene, and 100mL of N,N-dimethylformamide. The mixture was heated to 115°C for 2 days until the required amount of water was distilled. The flask was cooled to rt before adding 0.91g (0.0075 mol) allyl bromide. The reaction was heated to 50°C overnight, and the product precipitated in 500 mL of ice. It was filtered and air dried before being recrystallized from 50/50 (vol) hexane/methylene chloride to provide 0.62g (29%) white product: mp 190-2°C; MS m/z (M+) = 368.

### **Ethyl 2-allyloxy benzoate (28)**

In a 1L, 3 necked, round-bottomed flask equipped with a condenser, was placed 12.46g (0.075 mol) of ethyl salicylate **27**, 21.25g (0.154 mol) of  $\text{K}_2\text{CO}_3$ , and 385 mL of DMF. The solution was stirred under nitrogen for 30 min and 27.22g (0.225 mol) of allyl

bromide was added. The reaction was heated at 50°C for 3 d. The solution was cooled to rt and poured into 800 mL of ice. Methylene chloride (200 mL) was used to separate the organic material and was removed *in vacuo*. TLC (silica, 25/75 heptane/CH<sub>2</sub>Cl<sub>2</sub>) of the residual oil showed two products. Flash chromatography (silica, 25/75 heptane/CH<sub>2</sub>Cl<sub>2</sub>) was employed to separate the products and the solvent was removed *in vacuo* to yield 5.0g (32%) of an oil: IR (film) cm<sup>-1</sup> 3079 (aromatic C-H), 2983, 2935 (aliphatic C-H), 1725 (C=O), 1659 (alkene C=C), 1490, 1451 (aromatic C=C), 1301, 1250 (C-O-C); MS m/z (M<sup>+</sup>) = 206. Anal. Calcd. for C<sub>12</sub>H<sub>14</sub>O<sub>3</sub>: C, 69.90%; H, 6.80%. Found: C, 69.92%; H, 6.94%.

### **2-Allyloxybenzoic acid (29)**

In a 500 mL, 3-necked, round-bottomed flask equipped with a condenser was placed 15.0g (0.0727 mol) of ethyl 2-allyloxy benzoate **28**, 9.70g (0.243 mol) of NaOH, and 280 mL of a 50/50 (vol) ethanol/water solution. The reaction mixture was allowed to reflux under nitrogen overnight. On cooling, concentrated hydrochloric acid was added dropwise to precipitate a yellow product. This product was recrystallized from hexanes, filtered and dried to yield 4.08g (32%) of white crystals: mp 62-4°C; IR (KBr) cm<sup>-1</sup> 3200-2250 (O-H), 1699 (C=O), 1493-1410 (aromatic C=C); MS m/z (M<sup>+</sup>) = 178. Anal. Calcd. for C<sub>10</sub>H<sub>10</sub>O<sub>3</sub>: C, 64.40%; H, 5.60%. Found: C, 67.35%; H, 5.61%.

### **2,2-Bis(2-(2-allyloxyphenyl)-5-benzoxazolyl)-1,1,1,3,3,3-hexafluoropropane (31)**

In a polymerization flask equipped with an overhead stirrer and nitrogen inlet and outlet, was placed 1.0g (0.0056 mol) of 2-allyloxybenzoic acid **29**, 1.028g (0.0028 mol) of 2,2-bis(3-amino-4-hydroxyphenyl)-1,1,1,3,3,3-hexafluoropropane **30**, 13.44g PPSE, 1.91g (0.0224 mol) tributylamine, and 34 mL of o-dichlorobenzene. The mixture was

stirred and heated at 85°C for 18 h, 135°C for 18 h, and 165°C for 4 h. Precipitation in isopropyl alcohol yielded only a small amount of product which was used for analysis.

**2,2-Bis(2-(2-hydroxyphenyl)-5-benzoxazolyl)-1,1,1,3,3,3-hexafluoropropane (33)**

In a polymerization flask equipped with an overhead stirrer and nitrogen inlet and outlet, was added 8.01g (0.022 mol) 2,2-bis(3-amino-4-hydroxyphenyl)-1,1,1,3,3,3-hexafluoropropane **30**, 6.20g salicylic acid **32** (0.045 mol), and 45g of 83% poly(phosphoric acid). The reaction was heated at 160°C 1d and precipitated in water. The precipitate was filtered and washed with copious amounts of water to achieve neutral pH. It was filtered and dried under vacuum before being recrystallized from toluene to yield 7.46g (60%) off-white product mp 209-11°C: IR (KBr)  $\text{cm}^{-1}$  3077 (O-H), 1484, 1438 (aromatic C=C); MS  $m/z(M^+)$  = 570. Anal. Calcd. for  $\text{C}_{29}\text{H}_{16}\text{F}_6\text{N}_2\text{O}_4$ : C, 61.06%; H, 2.83%; N, 4.91%; F, 19.98%. Found: C, 61.91%; H, 2.94%; N, 4.59%; F, 18.67%.

**Bis(2-(2-allyloxyphenyl)-5-benzoxazolyl)-1,1,1,3,3,3-hexafluoropropane (31)**

In a 250mL, 3 necked, round-bottomed flask equipped with reflux condenser was placed 2.0g (0.0035 mol) bis(2-(2-hydroxyphenyl)-5-benzoxazolyl)-1,1,1,3,3,3-hexafluoropropane **33**, 1.053g (0.0076mol) potassium carbonate, 1.40g (0.011 mol) allyl bromide, and 50 mL of N,N-dimethylformamide. The reaction was heated to 50°C for 2 days, and poured into 500 mL of ice to precipitate the product. The product was filtered, dried, and recrystallized from isopropanol to yield 1.2g (52%) of tan product: mp 102-7°C (DSC); IR (KBr)  $\text{cm}^{-1}$  2962 (aliphatic C-H), 1479, 1453 (aromatic C=C); MS  $m/z(M^+)$  = 650. Anal. Calcd. for  $\text{C}_{35}\text{H}_{24}\text{N}_2\text{O}_4\text{F}_6$ : C, 64.62%; H, 3.72%; N, 4.31%; F, 17.52%. Found: C, 63.86%; H, 3.57%; N, 4.07%; F, 15.33%.



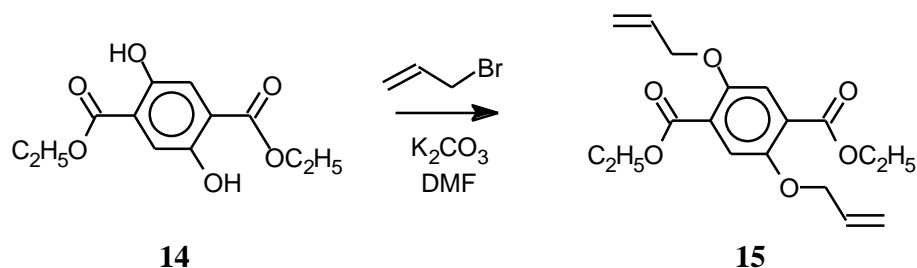
### Thermal Analysis

The model compounds **18**, **25**, and **31** were analyzed using Differential Scanning Calorimetry (DSC). Each sample was scanned at 10°C/min from rt to 200°C, and held there for 2 h. The sample was then cooled to rt and scanned at the same rate from rt to 400°C (600°C for **31**).

## RESULTS AND DISCUSSION

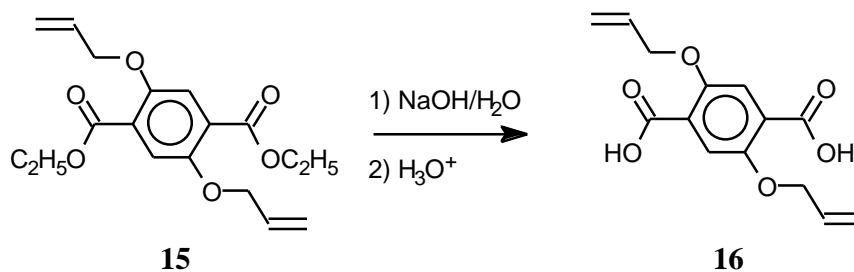
### Diallyloxybenzoxazole Model Compound Synthesis

The desired diallyloxybenzoxazole model compound required a multistep synthesis. Initially, diethyl 2,5-dihydroxyterephthalate **14** was reacted with allyl bromide and  $K_2CO_3$  in DMF to yield diethyl 2,5-di(allyloxy)terephthalate **15**. Evidence for this conversion is the disappearance



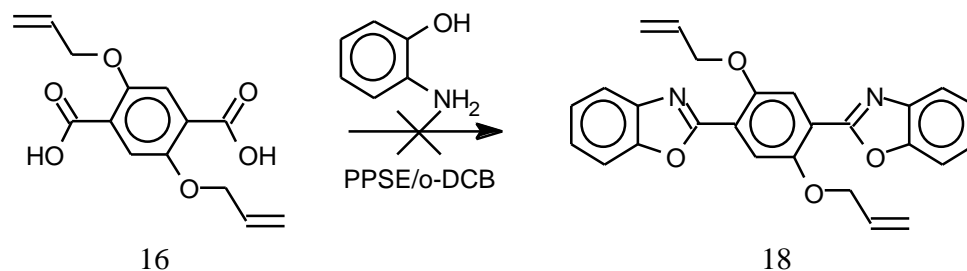
of the hydroxyl group absorption at  $3295\text{ cm}^{-1}$  in the IR spectrum (Figure 4) of **14**, and the presence of an ether group absorption at  $1705\text{ (C=O)}$ , and  $1201\text{ (C-O-C)}\text{ cm}^{-1}$  as well as an alkene (C=C) absorption at  $1650\text{ cm}^{-1}$  in the IR spectrum (Figure 5) of **15**. The mass spectrum of **15** indicated a molecular ion at 334 amu.

Compound **15** was then converted to the diacid, 2,5-di(allyloxy)terephthalic acid **16** employing NaOH in ethanol. The diacid **16** was characterized by the presence of a

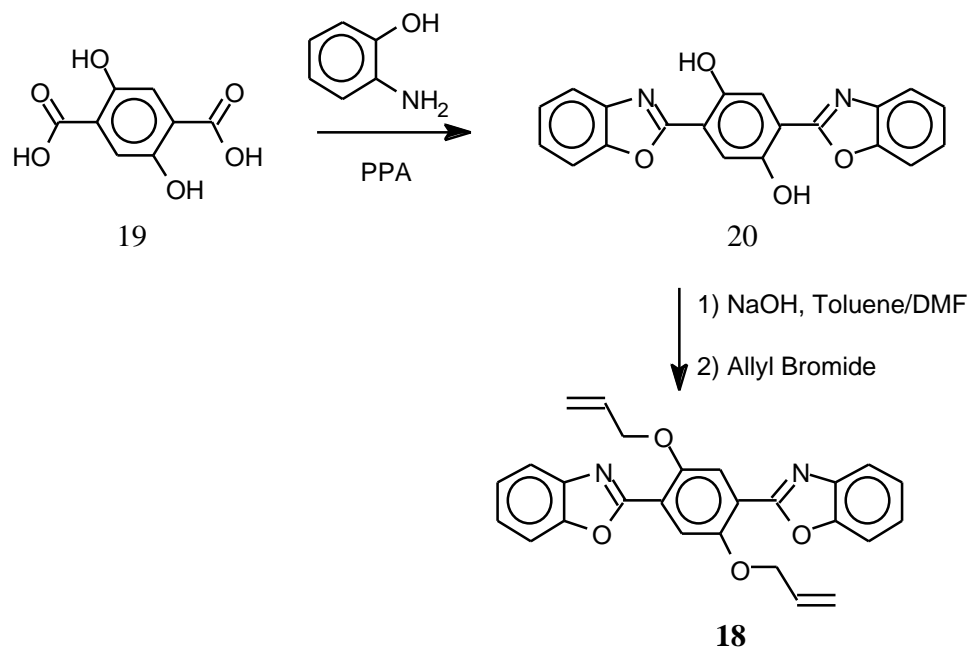


broad acid OH absorption at 3250-2250  $\text{cm}^{-1}$  and an acid carbonyl absorption at 1675  $\text{cm}^{-1}$  in the IR spectrum (Figure 6). The mass spectrum of **16** indicated a molecular ion at 278 amu.

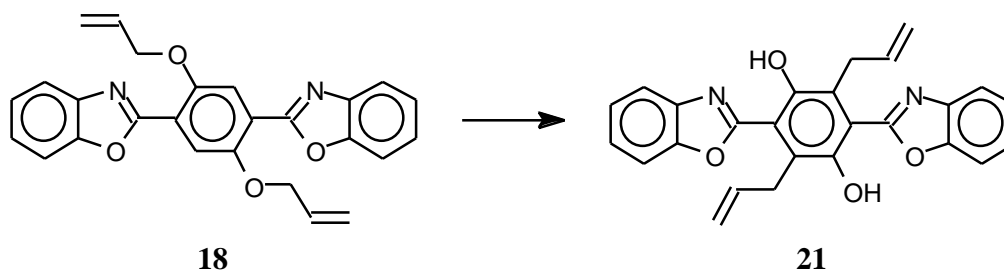
Acid **16** was reacted with 2-aminophenol **17** to produce 2,5-bis(2-benzoxazolyl)-1,4-di(allyloxy)benzene **18** model compound. No product was isolated from this reaction.



A post-reaction allyl addition was employed as an alternative method to obtain model compound **18** for subsequent thermal studies. In this approach the allyloxy groups are added as the final step, after the benzoxazole has been formed. The reaction of 2,5-dihydroxyterephthalic acid **19** with 2-aminophenol **17** was carried out in poly(phosphoric



acid) (PPA) to yield 2,5-bis(2-benzoxazolyl)-1,4-dihydroxybenzene **20**. Evidence for this is the disappearance of the broad acid OH absorption at  $3250 - 2250\text{ cm}^{-1}$  present in the IR spectrum of **19**, and the presence of an OH absorption at  $3129\text{ cm}^{-1}$  in the IR spectrum of **20** (Figure 7). The mass spectrum of **20** indicated a molecular ion at 344 amu. The reaction of **20** with sodium hydroxide followed by allyl bromide provided 2,5-bis(2-benzoxazolyl)-1,4-di(allyloxy)benzene **18** in moderate yield. Evidence for this conversion is the disappearance of the hydroxyl group absorption at  $3129\text{ cm}^{-1}$  in the IR spectrum (Figure 7) of **20**, and the presence of an ether group (C-O-C) absorption at  $1225\text{ cm}^{-1}$  as well as an aliphatic (C-H) absorption at  $2863\text{ cm}^{-1}$  in the IR spectrum (Figure 8) of **18**. The mass spectrum of **18** indicated a molecular ion at 424 amu.



The Claisen rearrangement for **18** to form **21** was shown by DSC analysis, and will be discussed in detail in a separate section. Elemental analysis results for all compounds synthesized are reported in Table 5 at the end of this section. The results for the diallyoxybenzoxazole model compound and relevant precursors are summarized below in Table 2.

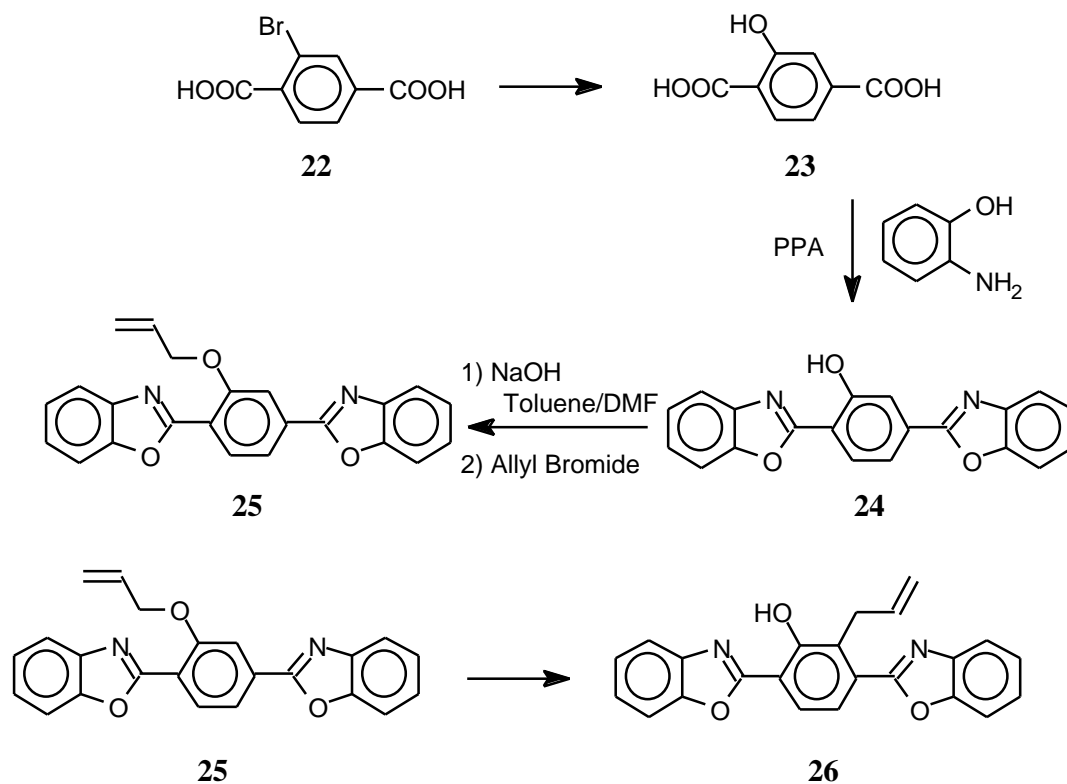
**Table 2.** Analytical Results for Diallyloxybenzoxazole Model Compound Synthesis (Compounds **15**, **16**, **18**, and **20**)

#	Yield	mp °C	MS (M+)	IR cm <sup>-1</sup>	NMR
<b>15</b>	48 %	40-1	334	3068 (C-H); 2980-2864 (C-H); 1705 (C=O); 1650 (C=C); 1508, 1459 (C=C); 1201 (C-O-C)	
<b>16</b>	80 %	168-70	278	3250-2250 (O-H); 1675 (C=O); 1447, 1502 (C=C); 1249, 1216 (C-O-C)	
<b>18</b>	51 %	222-3	424	3059, 3012 (C-H); 2863 (C-H); 1678 (C=C); 1552 (C=N); 1426 (C=C); 1225 (C-O-C)	
<b>20</b>	41 %	380-3	344	3129 (O-H); 1566 (C=N); 1502, 1451 (C=C)	

### Monoallyloxybenzoxazole Model Compound Synthesis

For comparison with model compound **18**, a monoallyloxybenzoxazole was prepared in the same post allyloxy addition as described above. Initially, 2-hydroxyterephthalic acid **23** was prepared from 2-bromoterephthalic acid **22** using the procedure given by Field and Engelhardt.<sup>12</sup> Acid **23** was then reacted with 2-aminophenol **17** in PPA to provide 2,5-bis(2-benzoxazolyl)-1-hydroxybenzene **24**. Evidence for **24** includes the disappearance of the broad acid OH absorption present at 3750 – 2250 cm<sup>-1</sup> in the IR spectrum of **23** (Figure 9), and the presence of an OH absorption at 3048 cm<sup>-1</sup> in the IR spectrum of **24**. The mass spectrum of **24** indicated a molecular ion at 328 amu. The allyl ether, 2,5-bis(2-benzoxazolyl)-1-allyloxybenzene **25** was prepared by the reaction of **25** with sodium hydroxide followed by allyl bromide. Compound **25** was characterized by the disappearance of the hydroxyl group absorption at 3048 cm<sup>-1</sup> in the IR spectrum (Figure 10) of **24**, and the appearance of an ether group

absorption at  $1245\text{ cm}^{-1}$  as well as an aliphatic C-H absorption at  $2921\text{ cm}^{-1}$  in the IR spectrum (Figure 11) of **25**. The mass spectrum of **25** indicated a molecular ion at 368 amu. Heating the model compound to  $200^{\circ}\text{C}$  should cause a Claisen rearrangement to occur to provide **26**. The results for the reaction resulting in **26** will be discussed in detail in a subsequent section.



The results for the monoallyloxybenzoxazole model compound synthesis are summarized in Table 3.

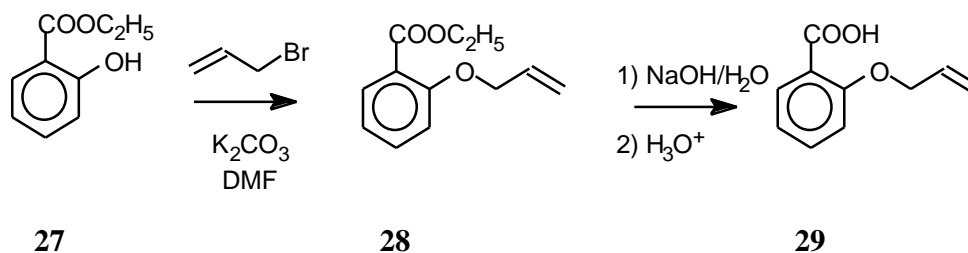
### 6F-benzoxazole Model Compound Synthesis

The final model compound synthesis also required a multi-step reaction sequence, quite similar to the synthetic scheme for **18**. Ethyl 2-allyloxybenzoate **28** was prepared by the reaction of ethyl salicylate **27** with allyl bromide in the presence of potassium carbonate. Evidence for **28** include the disappearance of the OH absorption at  $3153\text{ cm}^{-1}$

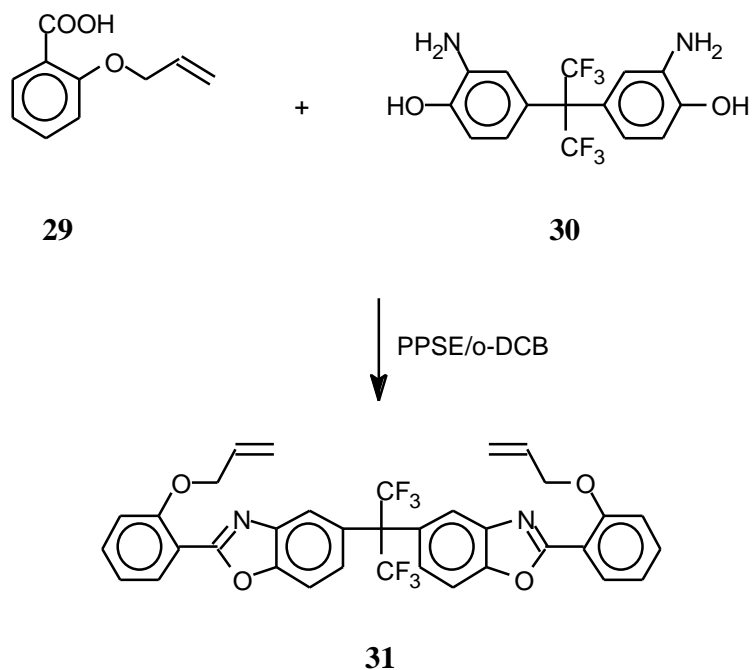
**Table 3.** Analytical Results for Monoallyloxybenzoxazole Model Compound Synthesis.

#	Yield (%)	mp °C	MS (M+)	IR cm <sup>-1</sup>	NMR
<b>24</b>	64	318-21	328	3048 (O-H); 1566 (C=N); 1496,1452 (C=C); 1247 (C- O-C)	
<b>25</b>	29	190-2	368	3060 (aromatic C-H); 2920 (aliphatic C-H); 1558 (C=N); 1452,1426 (aromatic C=C); 1245 (C-O-C)	

in the IR spectrum of **27**, and the presence of an ether (C-O-C) absorption at 1301 and 1250 cm<sup>-1</sup>, and aliphatic (C-H) at 2983 and 2935 cm<sup>-1</sup> from the IR spectrum of **28** (Figure 13). Hydrolysis of ethyl 2-allyloxybenzoate **28** with sodium hydroxide yielded 2-allyloxybenzoic acid **29**. Evidence for **29** is the broad acid OH absorption from 3200-2250 cm<sup>-1</sup> in the IR spectrum of **29** (Figure 14) and the mass spectrum of **29** which shows a molecular ion at 178 amu.



Acid **29** was then reacted with 2,2-bis(3-amino-4-hydroxyphenyl)-1,1,1,3,3,3-hexafluoropropane **30** to provide a very small amount of impure 2,2-bis(2-(2-allyloxyphenyl)-5-benzoxazolyl)-1,1,1,3,3,3-hexafluoropropane **31**. The mass spectrum for **31** showed a minor molecular ion at 314 amu, and a major molecular ion at 650. Due



to the poor quality, and insufficient amount of product obtained from this route, a post-reaction allyl ether formation was used to produce the desired model compound **31**. The bis(o-aminophenol), 2,2-bis(3-amino-4-hydroxyphenyl)-1,1,1,3,3,3-hexafluoropropane **30** was reacted with salicylic acid **32** in PPA to produce 2,2-bis(2-(2-hydroxyphenyl)-5-benzoxazolyl)-1,1,1,3,3,3-hexafluoropropane **33**. Evidence for **33** is the OH absorption at  $3077\text{ cm}^{-1}$  from the IR spectrum of **33** (Figure 15), and the mass spectrum which indicates a molecular ion at 570 amu. Compound **33** was reacted with allyl bromide in the presence of potassium carbonate to produce 2,2-bis(2-(2-allyloxyphenyl)-5-benzoxazolyl)-1,1,1,3,3,3-hexafluoropropane **31** in moderate yields. Evidence for this is the disappearance of the OH absorption present in **33**, and the presence of an aliphatic C-H absorption at  $2962\text{ cm}^{-1}$  in the IR spectrum of **31** (Figure 16). The mass spectrum of **31** showed a molecular ion at 650 amu.



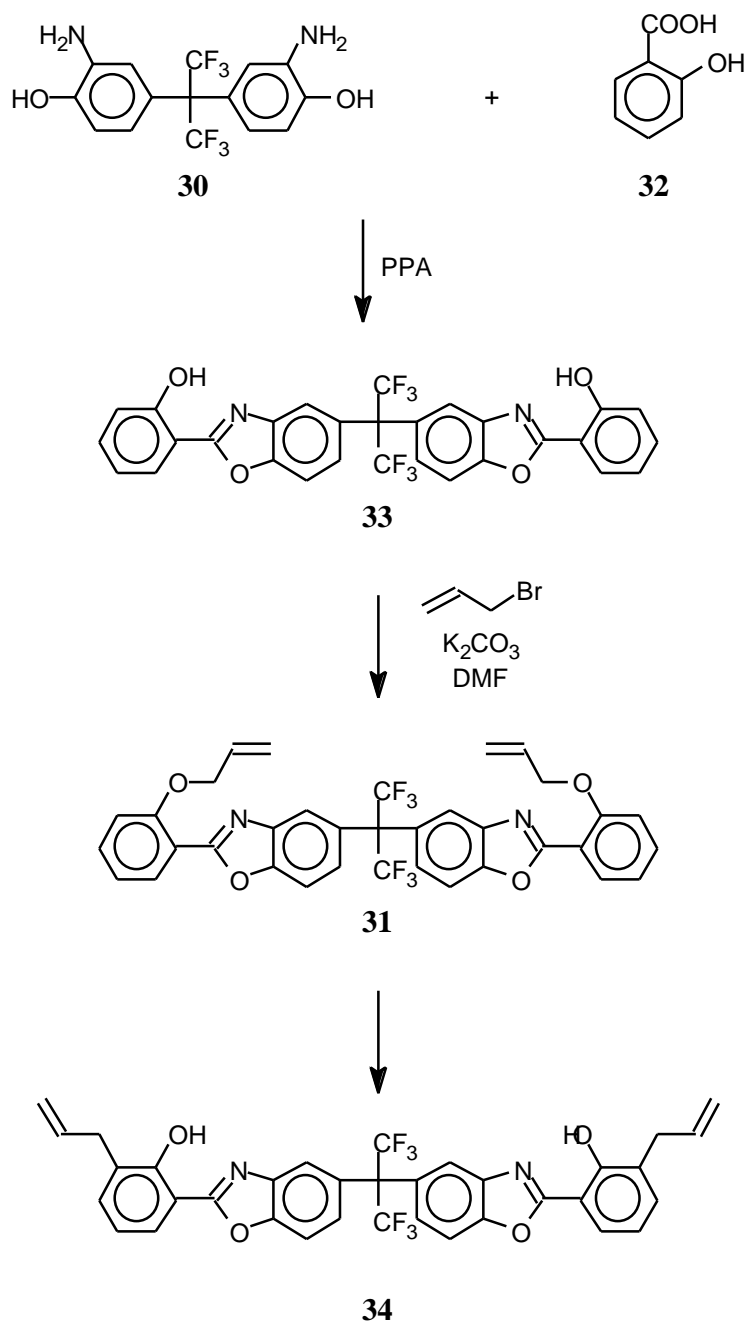


Table 4 summarizes the results of the synthesis of the 6F-benzoxazole model compound **31** and relevant precursors. Elemental analysis results for all of the compounds synthesized are given in Table 5 at the end of this section.

**Table 4.** Analytical Results for 6F-allyloxybenzoxazole Synthesis

#	Yield (%)	mp (°C)	MS (M+)	IR cm <sup>-1</sup>	NMR
<b>28</b>	32	oil	206	3079 (C-H); 2983, 2935 (aliphatic C-H); 1725 (C=O); 1659 (alkene C=C); 1490, 1452 (aromatic C=C); 1301, 1250 (C-O-C)	
<b>29</b>	32	62-4	178	3200-2250 (OH); 1699 (C=O); 1493-1410 (aromatic C=C)	
<b>31</b>	52	102-7	650	2962 (aliphatic C-H); 1479, 1453 (aromatic C=C)	
<b>33</b>	60	209-11	570	3077 (OH); 1484, 1438 (aromatic C=C)	

**Table 5.** Elemental Analysis Results for Benzoxazole Model Compounds and Precursors.

Compound	Carbon (%)		Hydrogen (%)		Nitrogen (%)	
	Theoretical	Found	Theoretical	Found	Theoretical	Found
<b>15</b>	64.66	64.55	6.63	6.65	-	-
<b>16</b>	60.43	60.33	5.07	4.81	-	-
<b>18</b>	73.60	72.97	4.75	4.63	6.60	6.42
<b>20</b>	69.76		3.51		8.13	
<b>24</b>	73.16		3.69		8.53	
<b>25</b>	75.00		4.38		7.60	
<b>28</b>	69.90	69.92	6.80	6.94	-	-
<b>29</b>	64.40	63.75	5.60	5.61	-	-
<b>31</b>	64.62	63.86	3.72	3.57	4.31	4.07
<b>33</b>	61.06	61.91	2.83	2.94	4.91	4.59

## Thermally Induced Claisen Rearrangement

The three model compounds synthesized, **18**, **25**, and **31** were each analyzed via differential scanning calorimetry (DSC) to determine whether the expected Claisen rearrangement would take place, and to observe what effects this would have upon the thermal properties of the compounds. Thermogravimetric analysis (TGA) was also performed on each sample to determine thermal stability. The initial DSC trace of **18** (Figure 17) showed an endotherm from 223 – 225°C. This is the melting point of the compound **18**, and corresponds well with the capillary melting point obtained for **18** (222-3°C). This is followed by an exotherm at 225 – 275°C. This may be due to the Claisen rearrangement and subsequent crystallization of the rearranged product **21**. This is followed by a second endotherm at 296 – 299°C, which would correspond to the melting point of the new product **21**. There is a final exotherm at 300 – 375°C, which could be attributed to the cure. When the sample was cooled to rt and then heated to 200°C and held for 2 h, the rescan (Figure 18) of this particular compound did not show any appreciable changes from the initial scan. It does appear that a Claisen rearrangement occurs with this compound, raising the melting point approx 75°C. The TGA of **18** in air (Figure 19) showed the onset of thermal degradation at 258°C, with 77 % weight loss at 312°C.

The DSC trace of **25** (Figure 23) showed an endotherm at 157 – 162°C, and another at 185 – 190°C. The first endotherm is probably attributed to the melting point of an impurity, and the second endotherm corresponds well to the capillary melting point obtained for **25** (190 – 192°C). An exotherm appears from approx 200 – 275°C, and another exotherm is present at approx 275 – 400°C. The initial exotherm could be

attributed to the Claisen rearrangement, and the second exotherm to the cure, or to degradation. The rescan of **25**, performed in the same manner as the previous samples, showed no appreciable endotherms or exotherms. The TGA in air of **25** showed the onset of degradation at 233°C, with 68% weight loss at 304°C. As with sample **25**, it is possible that The Claisen rearrangement reaction did not take place, or it is possible that the rearrangement product was formed but was amorphous, or degraded before melting.

The DSC of Compound **31** (Figure 20) showed an endotherm at 102 – 108°C, corresponding to the melting point of the compound, which compares well with the reported capillary melting point (102 - 107°C). This was followed by an exotherm from approx 200 – 300°C, which could be attributed to the Claisen rearrangement. A second smaller exotherm is observed at approx 350 – 400°C, possibly from the cure. A large exotherm begins at approx 425°C, probably due to decomposition. A rescan (Figure 21) of sample **31**, in the manner described for **18** above, showed the same two exotherms but no appreciable endotherms. (A small endotherm at is present at 64 – 70°C, perhaps due to an impurity or degradation product.) The absence of a second endotherm suggests that perhaps the Claisen rearrangement did not take place in this instance. However, it is possible that the rearrangement did take place, but could have formed an amorphous product, which would show no new melting point, or a product that degraded before melting. The TGA in helium of **31** (Figure 22) showed the onset of thermal degradation at 342°C, with a 60% weight loss at 375°C.

## **Conclusions and Future Work**

Regarding the synthesis of benzoxazoles containing pendant allyoxy groups, the traditional synthetic route in which the oxyally groups are added prior to benzoxazole

formation is not possible using the methods given in this work. It is possible to obtain benzoxazoles with pendant allyloxy groups in moderate yields, and of sufficient quality, using the post allyloxy addition approach.

From the DSC analysis of the three model compounds **18**, **25**, and **31** studied, it is not possible to conclusively determine whether a Claisen reaction has taken place, although it appears to do so in compound **18**, and is a possible interpretation of the results of **25** and **31**.

The simplest and most necessary suggestion for future work is to try the Claisen reaction on these products in solution so that they may be isolated and characterized by IR, Mass Spectrometry, and NMR etc., At the very least it should be possible to recover and characterize the product after DSC analysis. It would also be of value to run the thermal analysis on the precursors capable of rearrangement, like compounds **16** and **29**, to determine if they undergo the desired rearrangement. It should be noted that it is possible for the vinyl crosslinking to occur at a lower temperature than the Claisen rearrangement, causing no rearrangement.

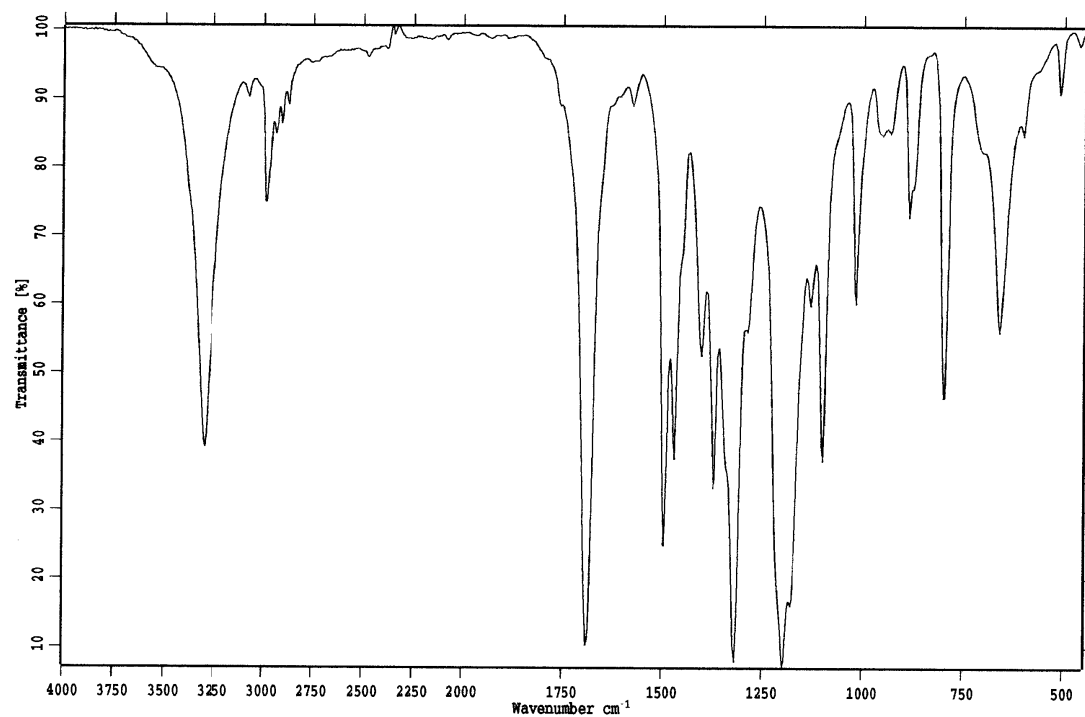


**Figure 4.** IR spectrum of 2,5-dihydroxyterephthalate.

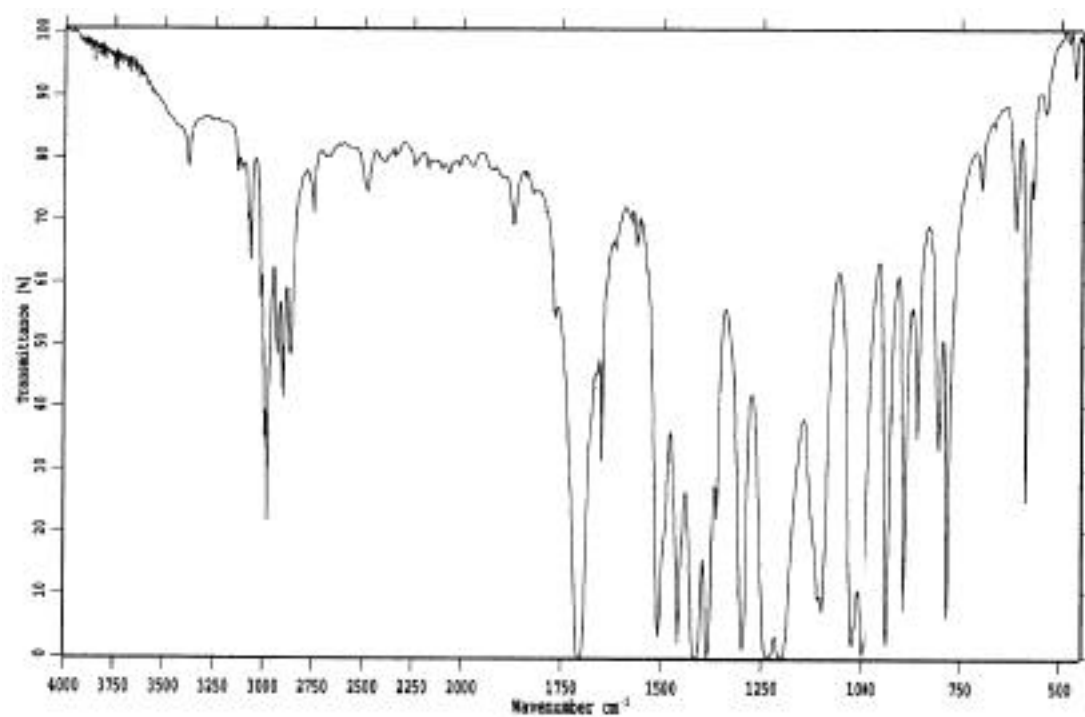


**Figure 5.** IR spectrum of diethyl 2,5-dihydroxyterephthalate.

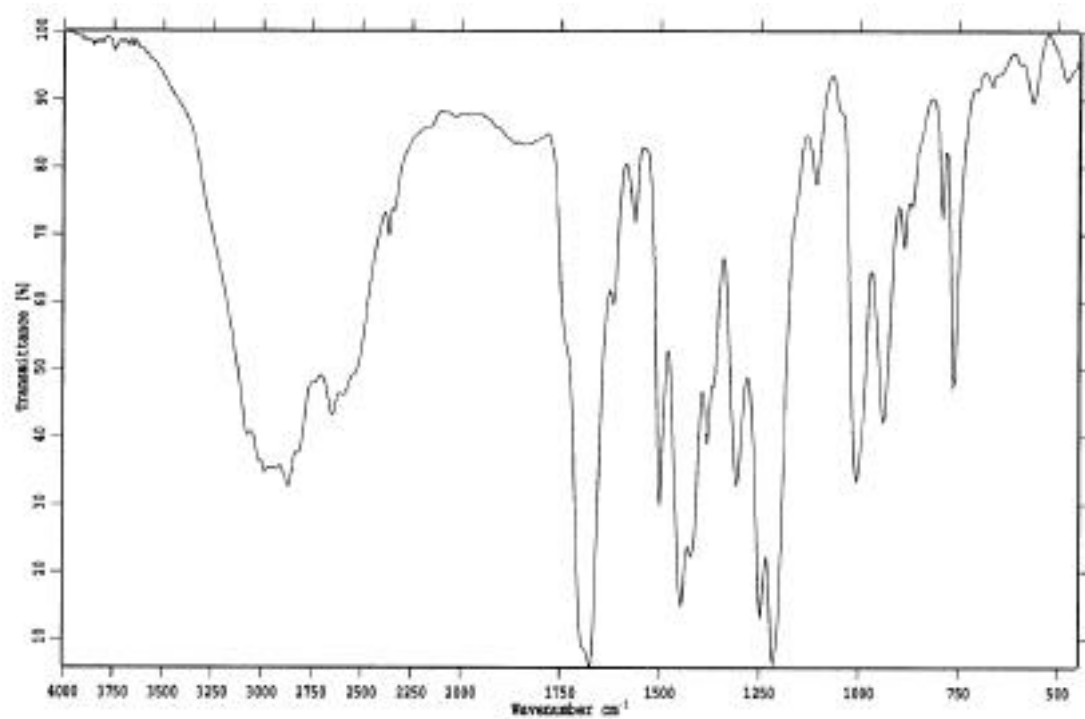


**Figure 6.** IR spectrum of 2,5-di(allyloxy)terephthalic acid.

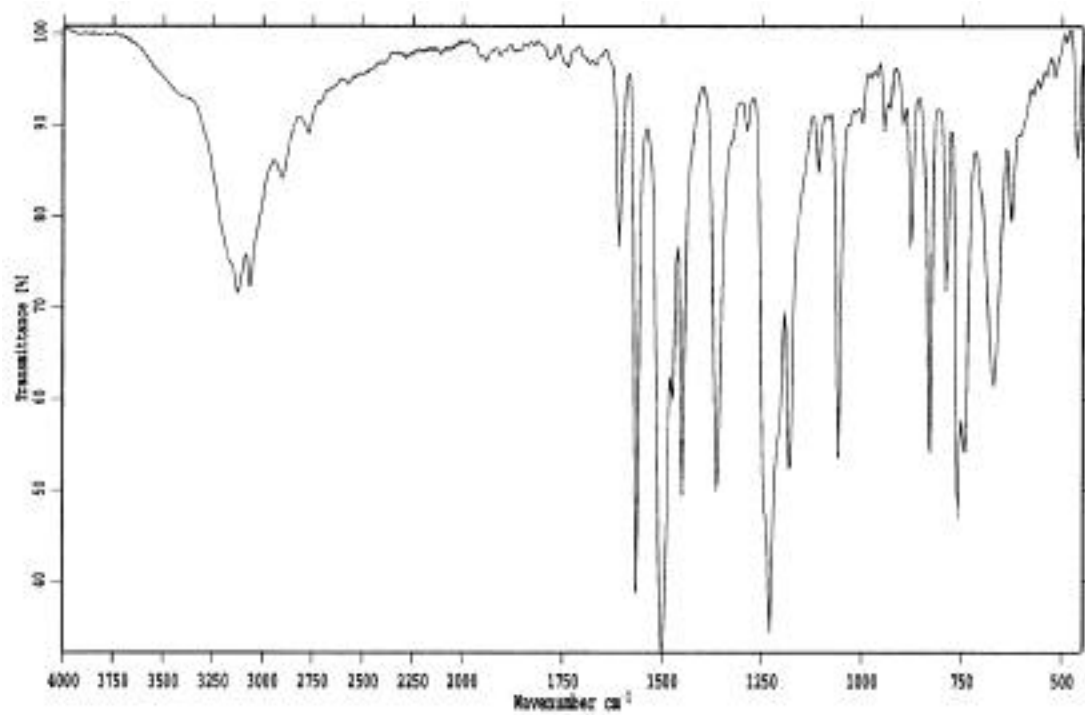


**Figure 7.** IR spectrum of 2,5-bis(2-benzoxazolyl)-1,4-dihydroxybenzene.

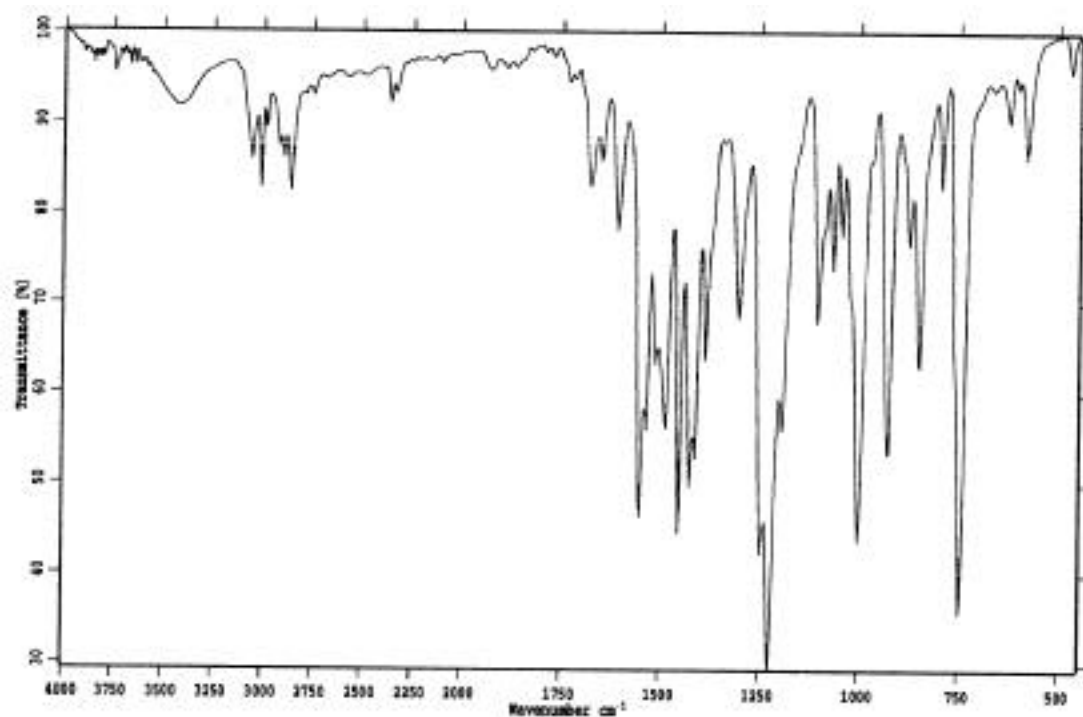


**Figure 8.** IR spectrum of 2,5-bis(2-benzoxazolyl)-1,4-di(allyloxy)benzene.

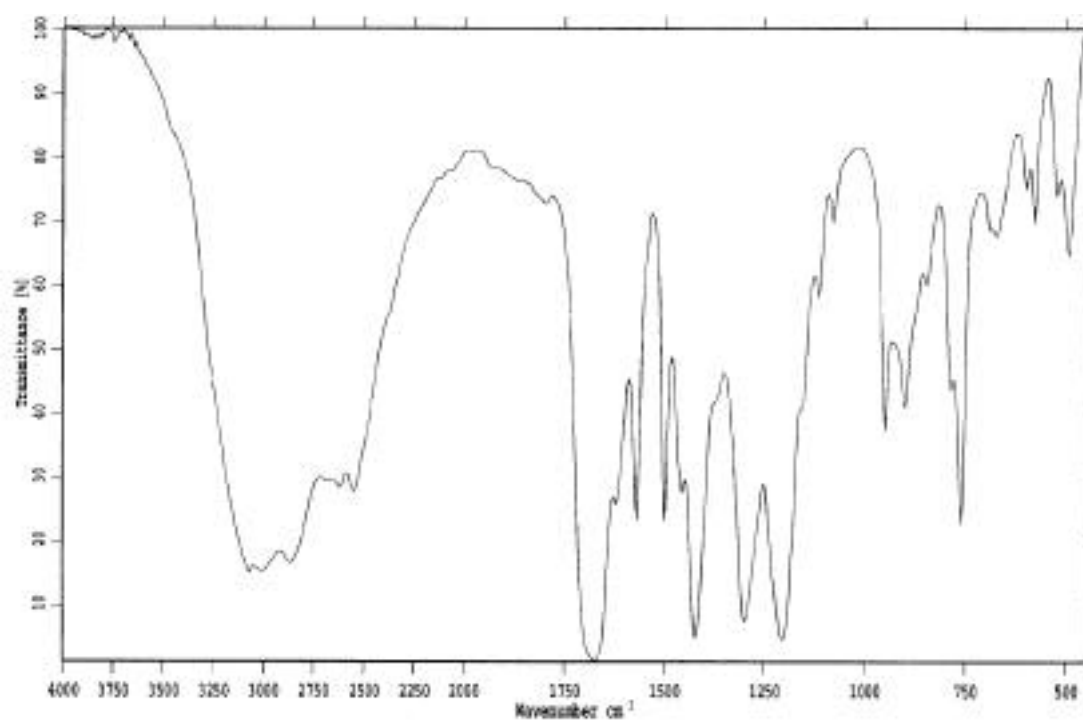


**Figure 9.** IR spectrum of 2-hydroxyterephthalic acid.



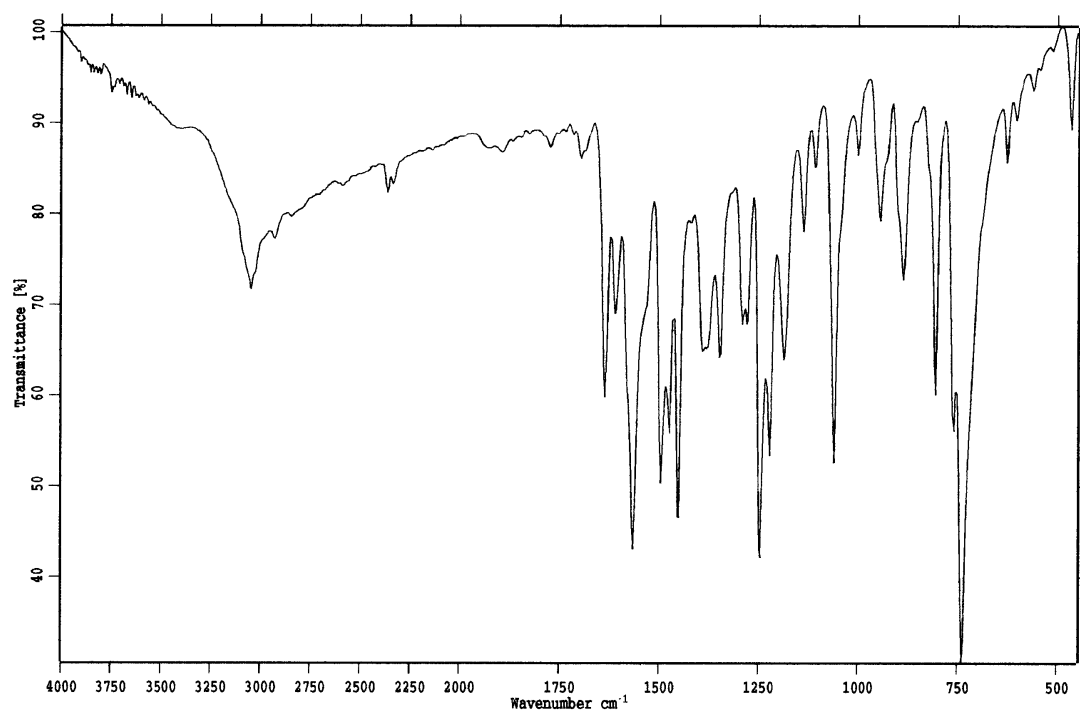


**Figure 10.** IR spectrum of 2,5-bis(2-benzoxazolyl)-1-hydroxybenzene.

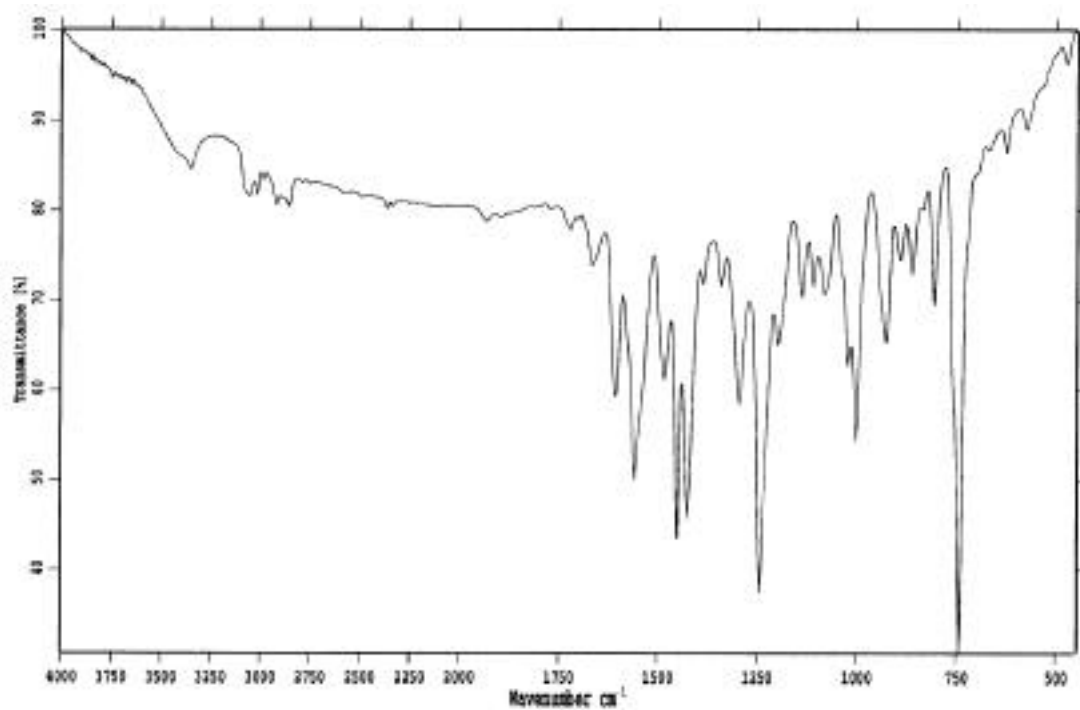


**Figure 11.** IR spectrum of 2,5-bis(2-benzoxazolyl)-1-allyloxybenzene.

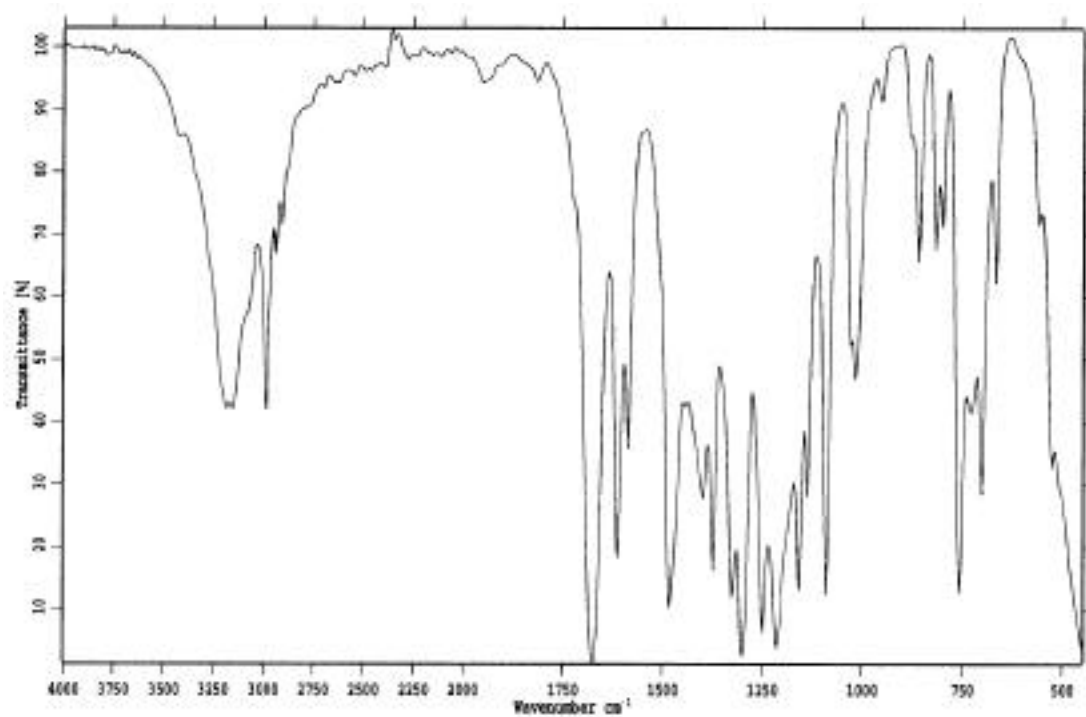


**Figure 12.** IR spectrum of ethyl salicylate.

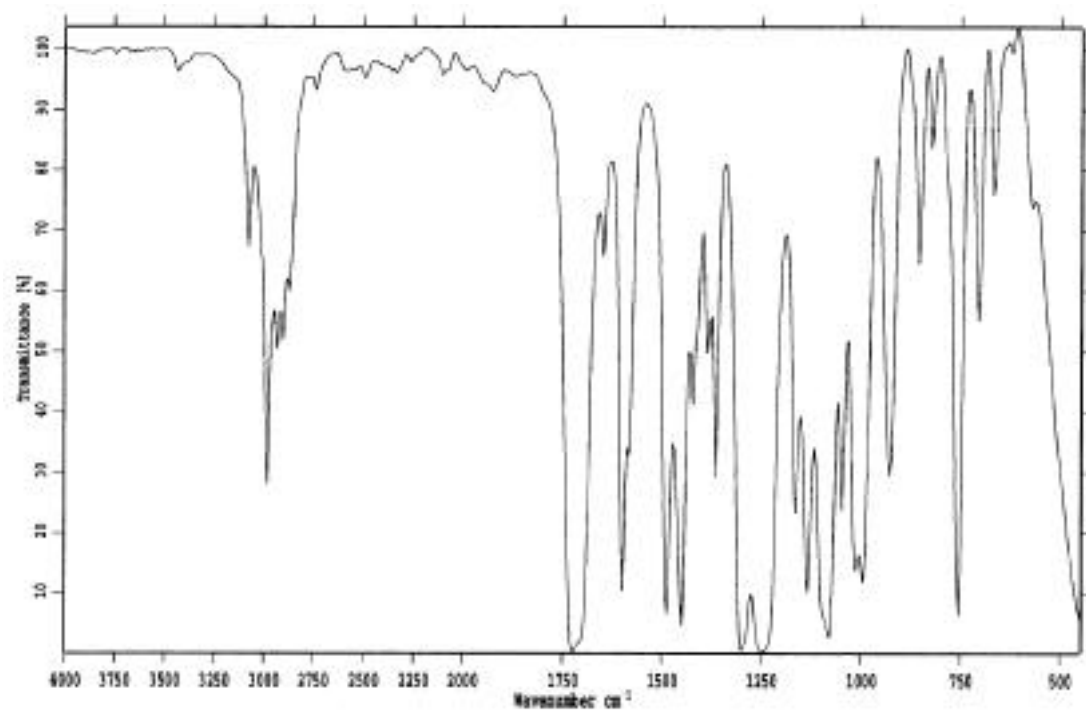


**Figure 13.** IR spectrum of ethyl 2-allyloxy benzoate.

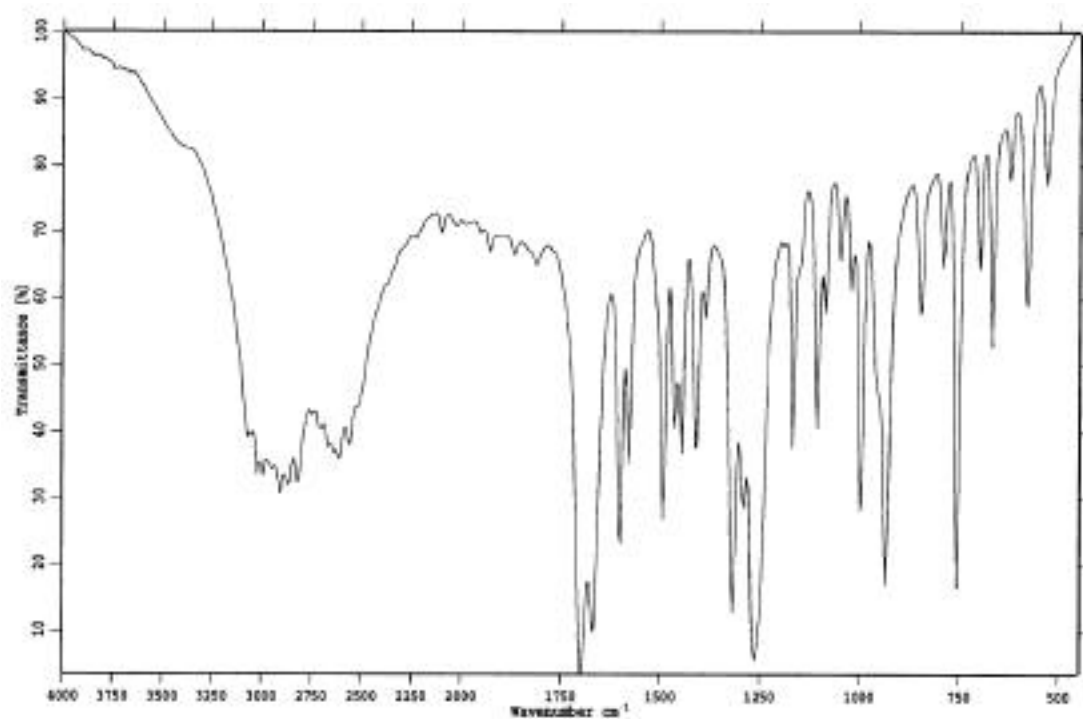


**Figure 14.** IR spectrum of 2-allyloxybenzoic acid.

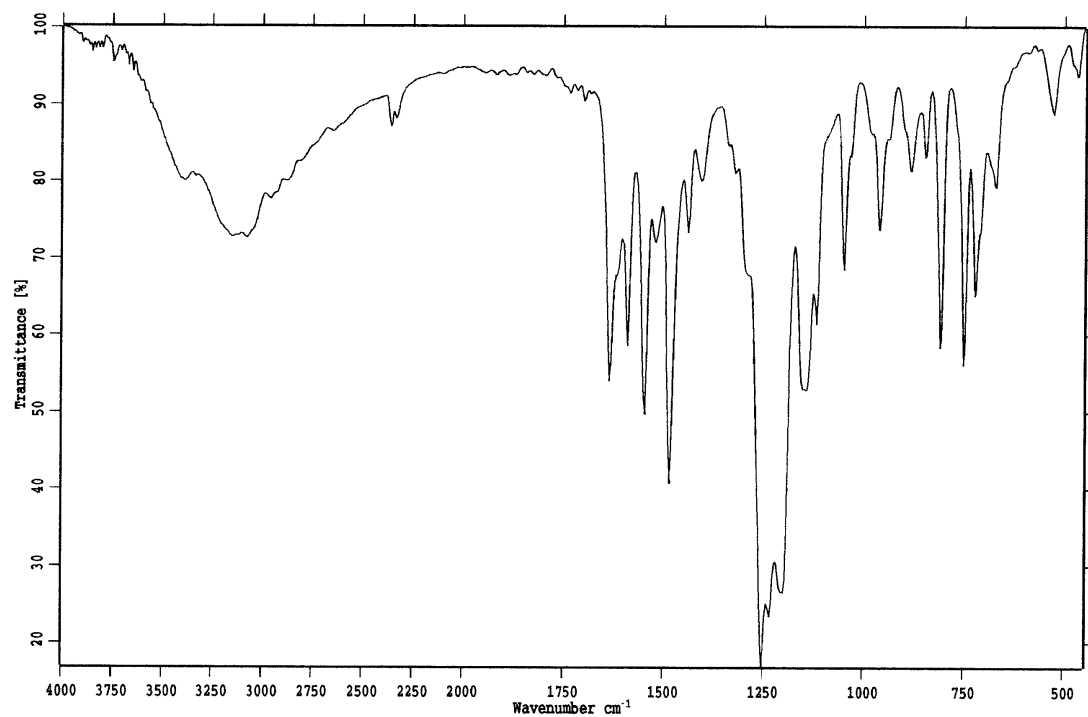


**Figure 15.** IR spectra of 2,2-bis(2-(2-hydroxyphenyl)-5-benzoxazolyl)-1,1,1,3,3,3-hexafluoropropane.

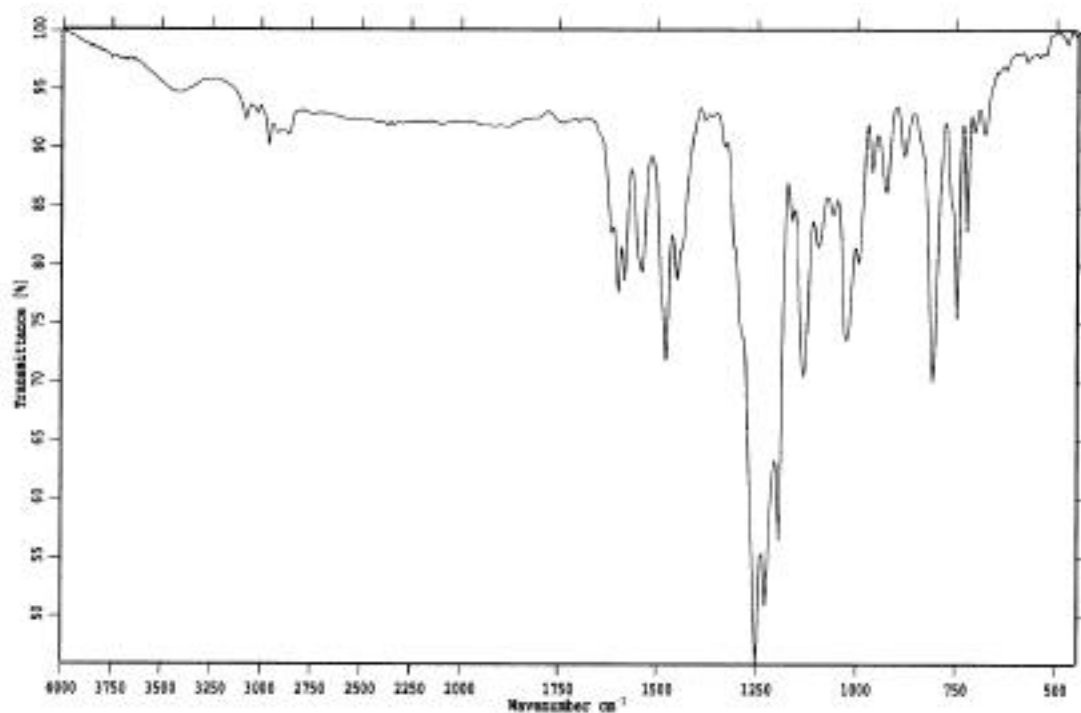


**Figure 16.** IR spectra of 2,2-bis(2-(2-allyloxyphenyl)-5-benzoxazolyl)-1,1,1,3,3,3-hexafluoropropane.

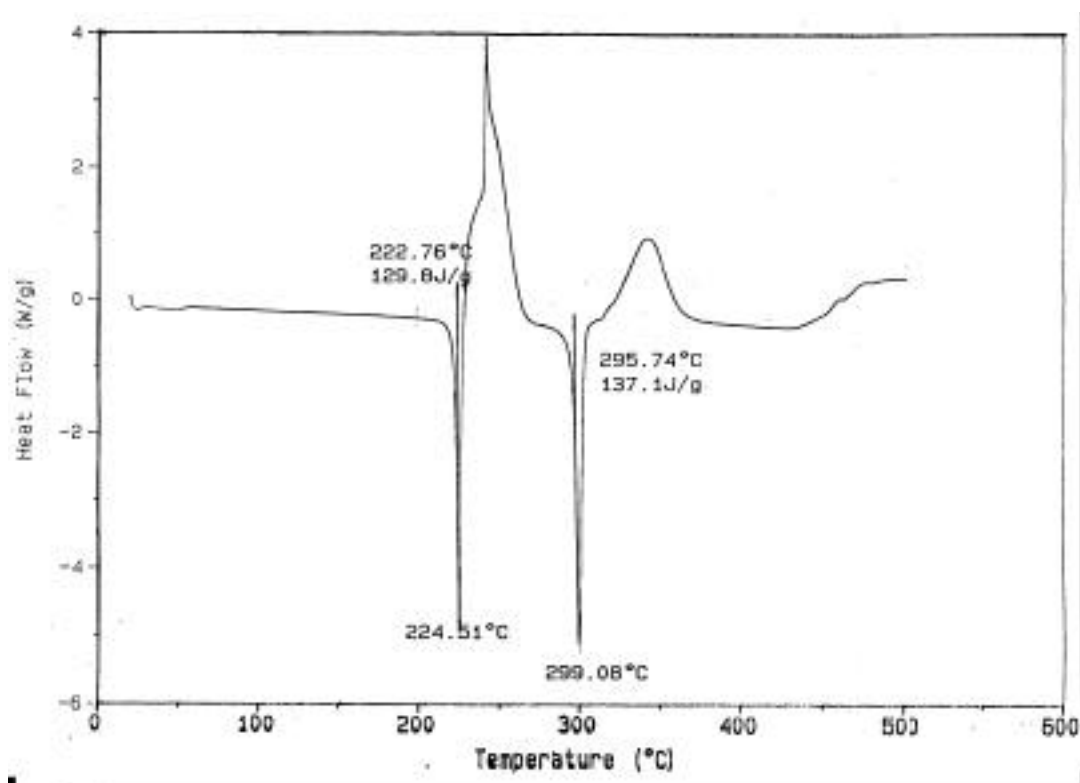


**Figure 17.** DSC scan of 2,5-bis(2-benzoxazolyl)-1,4-di(allyloxy)benzene.

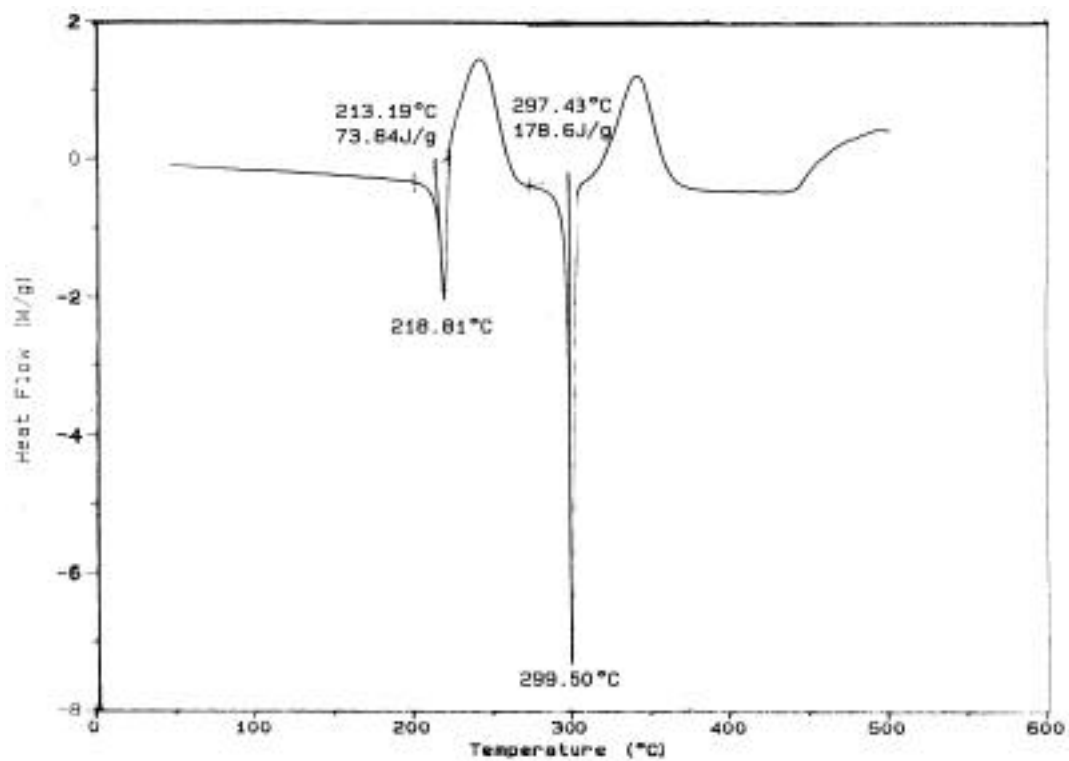


Figure 18. DSC rescan of 2,5-bis(2-benzoxazolyl)-1,4-di(allyloxy)benzene.

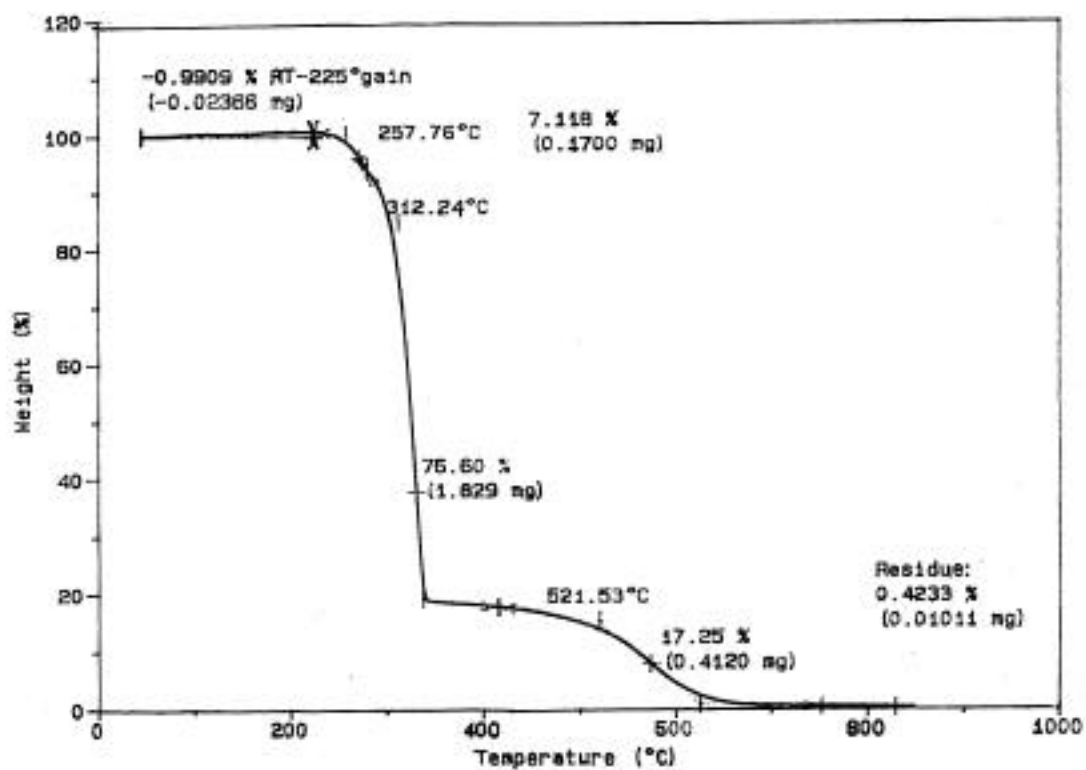
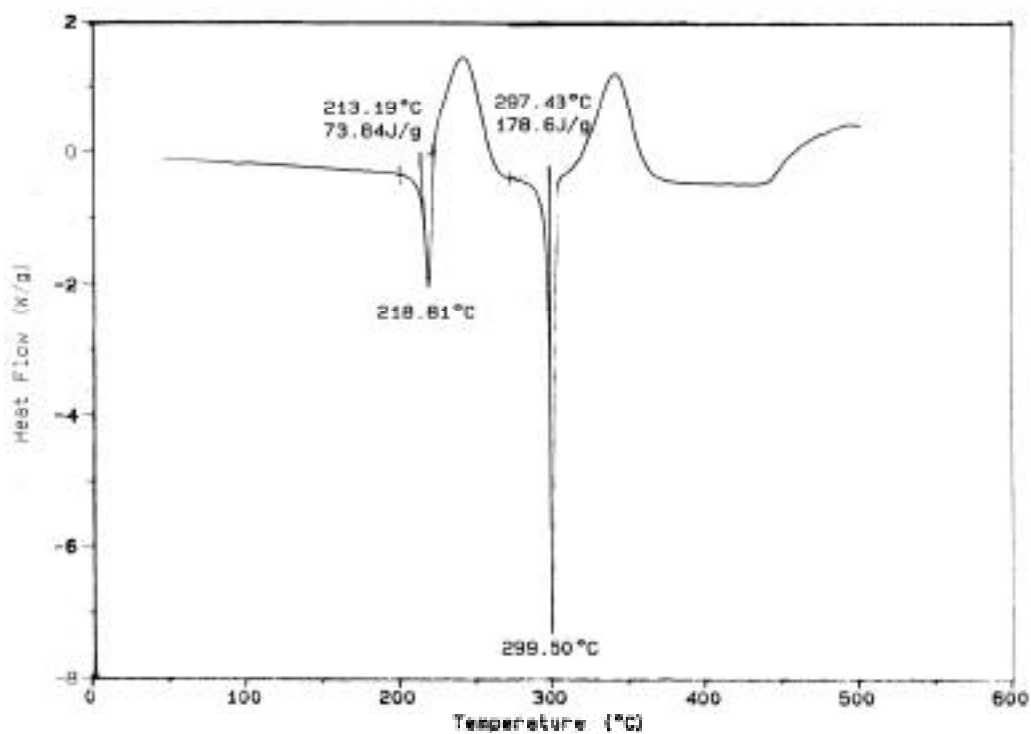
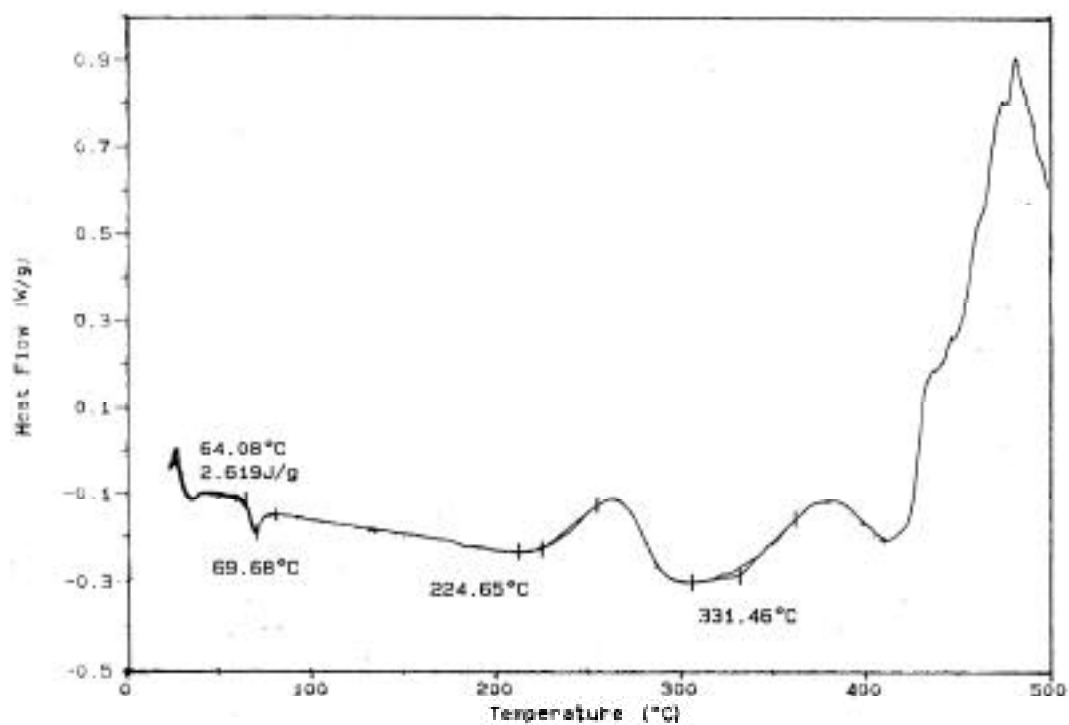


Figure 19. TGA in air of 2,5-bis(2-benzoxazolyl)-1,4-di(allyloxy)benzene.



**Figure 20.** DSC scan of 2,2-bis(2-(2-allyloxyphenyl)-5-benzoxazolyl)-1,1,1,3,3,3-hexafluoropropane



**Figure 21.** DSC rescan of 2,2-bis(2-(2-allyloxyphenyl)-5-benzoxazolyl)-1,1,1,3,3,3-hexafluoropropane.

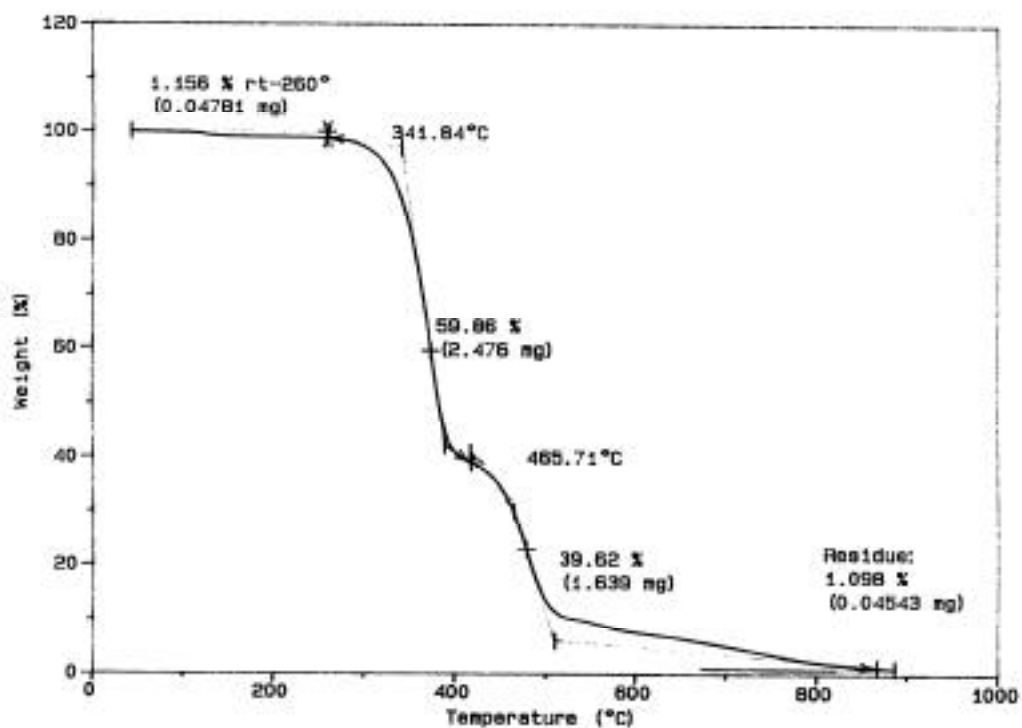


**Figure 22.** TGA in helium of 2,2-bis(2-(2-allyloxyphenyl)-5-benzoxazolyl)-1,1,1,3,3,3-hexafluoropropane

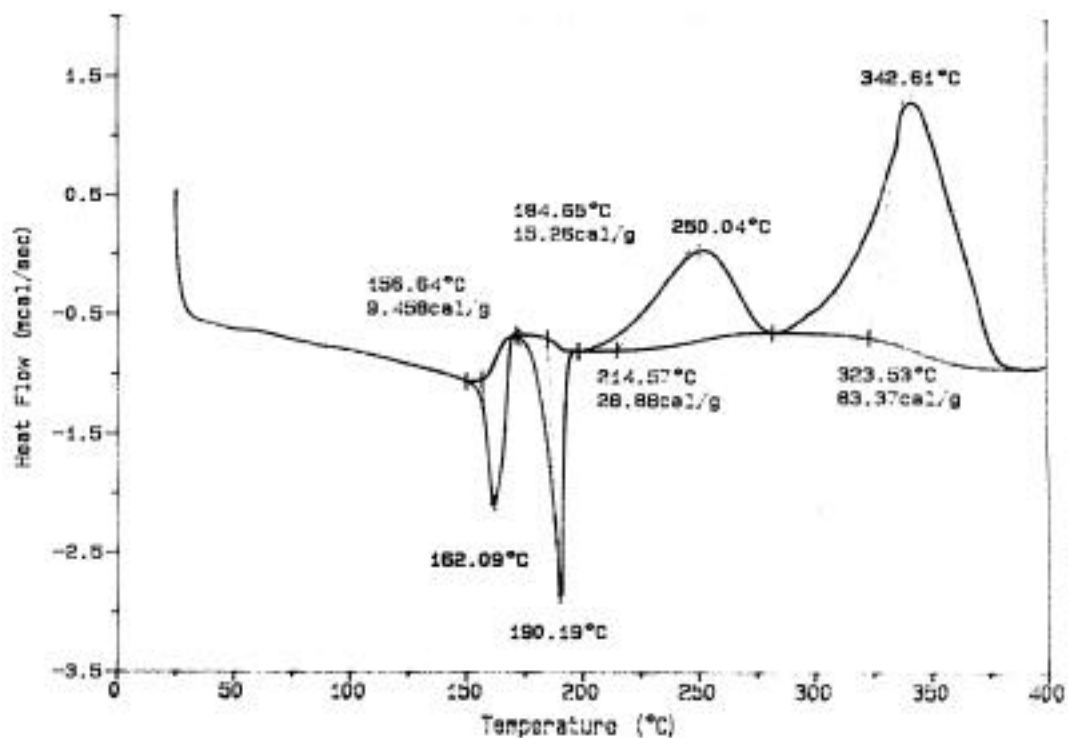


**Figure 23.** DSC scan of 2,5-bis(2-benzoxazolyl)-1-allyloxybenzene.

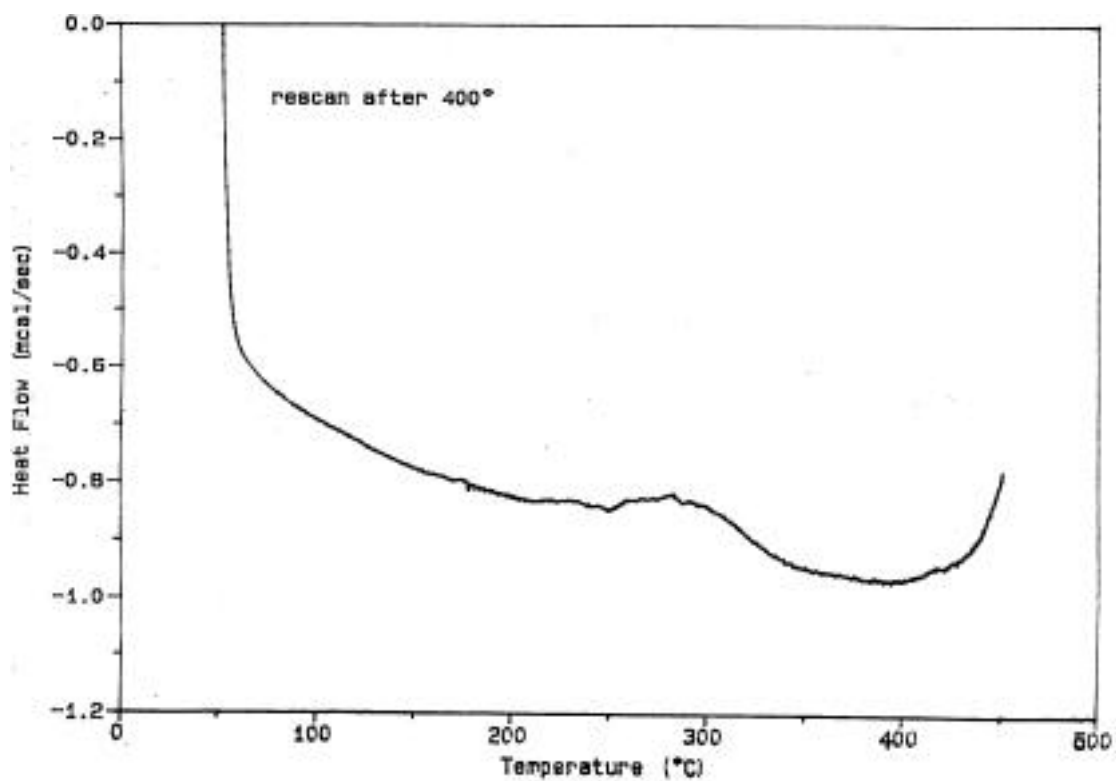


Figure 24. DSC rescan of 2,5-bis(2-benzoxazolyl)-1-allyloxybenzene

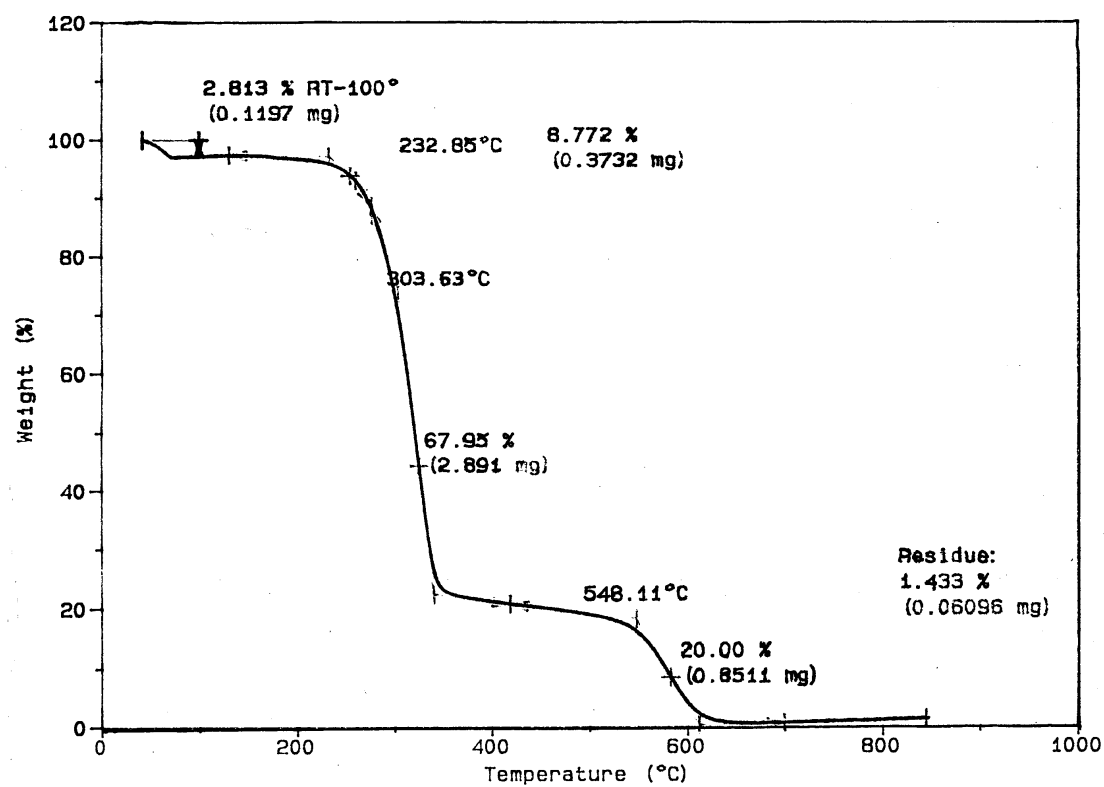


Figure 25. TGA in air of 2,5-bis(2-benzoxazolyl)-1-allyloxybenzene.



## REFERENCES

1. Arnold, F.E., Wright-Patterson Air Force Base, Dayton Ohio, Private Communication.
2. Lee, W.W. and Ho, P.S., *MRS Bulletin*, **1997**, 22(10), 19-23.
3. Dang, T.D., Mather, P.T., Alexander, M.D.Jr., Spry, R.J., and Arnold, F.E., *Polymer Preprints*, **1998**, 39(2), 804-5.
4. Ryan, E.T., McKerrow, A.J., Leu, J., and Ho, P.S., *MRS Bulletin*, **1997**, 22(10), 49-54.
5. List, R.S., Singh, A., Ralston, A. and Dixit, G., *MRS Bulletin*, 22 (10), **1997**, pp. 61-9.
6. Paul A. Tipler, Physics for Scientists and Engineers, 3<sup>rd</sup> Edition, Worth Publishers, New York, New York, **1991**, 690 - 724.
7. Carter, K.R., Hedrick, J.L., Richter, R., Hawker, C.J., et al, *Polymer Preprints*, **1996**, 37(2), 787-8.
8. Hedrick, J.L., Hawker, C.J., and DiPetro, R., et al., *Polymer*, **1995**, 36(25), 4855-66.
9. Hedrick, J., Russell, L.D., Hoffer, D., and Wakharker, V., *Polymer*, **1993**, 34(22), 4717-26.
10. Dang, T.D., Mather, P.T., Alexander, M.D.Jr., Spry, R.J., and Arnold, F.E., Wright Patterson Air Force Base Materials Laboratory, Dayton, Ohio, Private Communication.
11. Advanced Organic Chemistry: Reactions, Mechanisms and Structures, 4<sup>th</sup> edition, John March Ed., John Wiley & Sons Inc., New York, **1992**, **1136-41**.
12. Field, L., Engelhardt, P.R., *Journal of Organic Chemistry*, **1970**, 35, 3647.

## **VITA**

Leslie K. Hutson was born on September 3, 1971 in Dayton, Ohio. She completed her undergraduate degree at Wright State University, Dayton, Ohio, receiving a Bachelor of Science Degree in Chemistry in 1994. Leslie expects to receive her Master of Science degree in Organic Chemistry in December of 1999.